Atmos. Chem. Phys., 13, 869–894, 2013
www.atmos-chem-phys.net/13/869/2013/
doi:10.5194/acp-13-869-2013

Atmospheric Chemistry and Physics

Aerosol decadal trends – Part 1: In-situ optical measurements at GAW and IMPROVE stations

M. Collaud Coen[1], E. Andrews[2,3], A. Asmi[4], U. Baltensperger[5], N. Bukowiecki[5], D. Day[6], M. Fiebig[7], A. M. Fjaeraa[7], H. Flentje[8], A. Hyvärinen[11], A. Jefferson[2], S. G. Jennings[9], G. Kouvarakis[10], H. Lihavainen[11], C. Lund Myhre[7], W. C. Malm[6], N. Mihapopoulos[10], J. V. Molenar[12], C. O'Dowd[9], J. A. Ogren[3], B. A. Schichtel[13], P. Sheridan[3], A. Virkkula[4], E. Weingartner[5], R. Weller[14], and P. Laj[15]

[1]Federal Office of Meteorology and Climatology, MeteoSwiss, 1530 Payerne, Switzerland
[2]University of Colorado, CIRES, Boulder, Colorado, 80305, USA
[3]National Oceanic and Atmospheric Administration, Earth System Research Laboratory, Boulder, Colorado, 80305, USA
[4]Department of Physics, University of Helsinki, P.O. Box 64, Helsinki, Finland
[5]Paul Scherrer Institute, Laboratory of Atmospheric Chemistry, Villigen PSI, 5232, Switzerland
[6]Colorado State University, Cooperative Institute for Research in the Atmosphere, Fort Collins, CO 80523, USA
[7]NILU – Norwegian Institute for Air Research, Instituttveien 18, 2027 Kjeller, Norway
[8]German Weather Service, Meteorological Observatory Hohenpeissenberg, Albin-Schwaiger-Weg 10, 82383 Hohenpeißenberg, Germany
[9]School of Physics, National University of Ireland Galway, Galway, Co. Galway, Ireland
[10]Environmental Chemistry Processes Laboratory, Dept. of Chemistry, University of Crete, 71003 Heraklion Crete, Greece
[11]Finnish Meteorological Institute, Erik Palmenin aukio 1, 00560 Helsinki, Finland
[12]Air Resource Specialists, Inc., 1901 Sharp Point Drive, Suite E; Ft. Collins, CO 80525, USA
[13]National Park Service, Fort Collins, CO 80523, USA
[14]Alfred-Wegener-Institute for Polar and Marine Research, Am Handelshafen 12, 27570 Bremerhaven, Germany
[15]UJF-Grenoble 1/CNRS, LGGE UMR 5183, 38041 Grenoble, France

Correspondence to: M. Collaud Coen (martine.collaudcoen@meteoswiss.ch)

Received: 25 July 2012 – Published in Atmos. Chem. Phys. Discuss.: 20 August 2012
Revised: 4 December 2012 – Accepted: 4 December 2012 – Published: 22 January 2013

Abstract. Currently many ground-based atmospheric stations include in-situ measurements of aerosol physical and optical properties, resulting in more than 20 long-term (> 10 yr) aerosol measurement sites in the Northern Hemisphere and Antarctica. Most of these sites are located at remote locations and monitor the aerosol particle number concentration, wavelength-dependent light scattering, backscattering, and absorption coefficients. The existence of these multi-year datasets enables the analysis of long-term trends of these aerosol parameters, and of the derived light scattering Ångström exponent and backscatter fraction. Since the aerosol variables are not normally distributed, three different methods (the seasonal Mann-Kendall test associated with the Sen's slope, the generalized least squares fit associated with an autoregressive bootstrap algorithm for confidence intervals, and the least-mean square fit applied to logarithms of the data) were applied to detect the long-term trends and their magnitudes. To allow a comparison among measurement sites, trends on the most recent 10 and 15 yr periods were calculated. No significant trends were found for the three continental European sites. Statistically significant trends were found for the two European marine sites but the signs of the trends varied with aerosol property and location. Statistically significant decreasing trends for both scattering and absorption coefficients (mean slope of $-2.0\,\%\,\mathrm{yr}^{-1}$) were found for most North American stations, although positive trends were found for a few desert and high-altitude sites. The difference in the timing of emission reduction policy for the Europe and US continents is a likely explanation for the decreasing trends in aerosol optical parameters found for most American

Published by Copernicus Publications on behalf of the European Geosciences Union.

sites compared to the lack of trends observed in Europe. No significant trends in scattering coefficient were found for the Arctic or Antarctic stations, whereas the Arctic station had a negative trend in absorption coefficient. The high altitude Pacific island station of Mauna Loa presents positive trends for both scattering and absorption coefficients.

1 Introduction

Since the 1970's, aerosols have been recognized as an important atmospheric constituent and an active climate forcing agent (Charlson et al., 1992). The latest IPCC report yields an overall aerosol direct radiative forcing (RF) of $-0.5 \pm 0.4\,\mathrm{W\,m^{-2}}$ globally but this value conceals regional and local conditions that can lead to much stronger or weaker forcing (IPCC, 2007). The term "aerosol" encompasses a wide range of particle types having different compositions, sizes, shapes, and optical properties. Long-term measurements are the only possible approach for detection of change in atmospheric composition resulting from either changes in natural or anthropogenic emissions, and/or changes in atmospheric processes and sinks. The lifetime of atmospheric aerosols is on the order of days to weeks. Given their short lifetime, the spatial and temporal variability of aerosol properties is extremely high due to the wide variety of aerosol sources and types, the spatial non-uniformity and intermittent nature of aerosol sources and sinks, and the chemical and microphysical processing that occurs in the atmosphere.

Ground-based, in-situ measurements placed in areas away from emission sources such as EMEP (European Monitoring and Evaluation Programme), IMPROVE (Interagency Monitoring of Protected Visual Environments) and World Meteorological Organisation's (WMO) GAW (Global Atmosphere Watch) sites are most suited for studying the atmospheric spatial and temporal variability of aerosol properties as well as climate relevant changes and trends in the atmospheric composition of background air masses. Implementation of systematic measurements of aerosol properties at sites with regional to global representativity (Henne et al., 2010) began in the mid-1970's at several remote locations including the original NOAA baseline observatories (South Pole, American Samoa, Mauna Loa, and Point Barrow) (Bodhaine, 1983), Cape Grim (Gras, 1990), Zeppelin (Joranger and Ottar, 1984) and Mace Head (O'Connor et al., 2008). In the mid-1980's, the impact of long-range pollution transport on ecosystems and visibility drove the establishment of the IMPROVE (2006) program in the US (Malm et al., 1994; EMEP, 2012; Tørseth et al., 2012). While both programs supported implementation of sites indicative of the regional aerosol background, IMPROVE emphasized aerosol properties related to visibility (light scattering, light extinction, and chemical composition) whereas EMEP sites had a stronger development towards air quality and aerosol chemistry monitoring.

In the 1990's, a number of additional organisations initiated systematic aerosol monitoring activities in remote locations, often led by quasi-independent initiatives. Increased awareness of the impact of aerosols on climate radiative forcing led to measurement of an extended suite of aerosol properties (e.g. optical properties). Since the early 2000's a number of papers have provided overviews of aerosol physical and optical properties, for the European continent (Putaud et al., 2004; Van Dingenen et al., 2004; Asmi et al., 2011) and elsewhere (Delene and Ogren, 2002; Spracklen et al., 2010; Andrews et al., 2011; Malm et al., 1994). Networking of the different sites was strengthened under the European Commission (EC) funded programs CREATE, EUSAAR, and now ACTRIS, which has also improved the data quality and access considerably. Since the mid-2000's there has been a continued increase in the number of measurement sites as a response to both a clear demand from an expanding user community and the evolution of air quality (AQ) regulations to better control regional background levels. As a consequence, the availability of continuous records from regionally representative ground-based sites has increased in the last decade (there are currently 29 and 52 sites making long-term, continuous light absorption and scattering measurements listed in the EBAS data base (http://ebas.nilu.no), respectively) although the sparse coverage over some regions of the globe remains problematic (Laj et al., 2009).

Indication of decreasing or increasing trends in atmospheric composition is essential, not only for our knowledge of global to regional cycling of atmospheric constituents and natural and anthropogenic changes, but also to validate past and present emission inventories, and to test validity of models at different scales. This is particularly true for aerosol species in order to quantify the effectiveness of past emission abatement strategies implemented in various countries and the influence of these on aerosol radiative forcing. The existence of long-term measurement networks and multi-year to multi-decade data sets enables the analysis of long-term trends in aerosol optical and physical parameters and the correlation of these trends with changes in other aerosol parameters.

Long-term trend analyses (as opposed to seasonal or diurnal trends) of various aerosol and aerosol-related parameters have been reported previously in the literature. Some examples include trends in visibility (e.g. Mahowald et al., 2007; Stjern et al., 2011), aerosol optical depth (e.g. Zhang and Reid, 2010; Augustine et al., 2008; Xia, 2011, Junker et al., 2006), aerosol chemistry (e.g. Weller et al., 2011; Sorooshian et al., 2011; Quinn et al., 2007, 2009; Manktelow et al., 2007; Tørseth et al., 2012; Hand et al., 2012), number and mass concentration (e.g. Murphy et al., 2011; EMEP, 2010; Barmpadimos et al., 2011; Yu et al., 2012) and solar radiation (global dimming/brightening) (e.g. Wild, 2009, 2012). Modeled trends in aerosol properties based on

emissions estimates have also been compared to observations of long-term aerosol measurements (e.g. Leibensperger et al., 2012; Pozzoli et al., 2011; Streets et al., 2009; Roy et al., 2007). Typically, when statistically significant (s.s.) trends were identified in these papers, they could be related to specific changes in aerosol/aerosol precursor sources, e.g. to the effects of air pollution control strategies. For example, Barmpadimos et al. (2011) showed that decreases in PM_{10} in Swiss urban areas were related to strategies for reducing traffic emissions. Studies that analyzed trends over large areas (continental to global scale) found some regional differences in long-term trends (Zhang and Reid, 2010).

Detecting long-term trends of aerosol variables of interest to climate studies from in-situ ground based monitoring station is not trivial. This is due both to availability of reliable instruments suited for monitoring activities and to the difficulty of sustaining long-term observations of atmospheric composition. Data quality, changes in measurements, and natural variability were observed to cause problems with several of the long-term trend analyses mentioned above (e.g. Streets et al., 2009; Zhang and Reid, 2010; Mahowald et al., 2007), consistent with the potential problem areas cited by Weatherhead et al. (1998). The challenge of detecting trends of a signal affected by high natural variability on time scales ranging from years to hours can be overcome by using long time series. At present, however, and for the reasons explained above, measurement records of core aerosol climate variables (absorption and scattering coefficients, single-scattering albedo, number and size distribution) rarely exceed more than 20 yr for the longest time-series with few exceptions (e.g. number concentration at South Pole and Mauna Loa measured since 1974 and 1975, respectively).

The uncertainties caused by changes and biases in measurement methodology have also been a major limitation for deriving statistically relevant trends for these parameters. Trend analyses can only be performed on time series without break points or on homogenized time series that account for changes in the measurement conditions (relocations, instrument repair/upgrades, inlet changes, etc.). Homogenized data sets have been developed for the present study and for the associated study on number concentration and size distribution (Asmi et al., 2013) but not necessarily for all recently published papers. Additionally there are methodological problems – for example, it is statistically inappropriate to use statistical methods designed for normally distributed data on data that are not normally distributed (i.e. most aerosol parameters). Autocorrelation in the data is another sensitive problem that has to be carefully addressed when long-term trend analysis are estimated. In addition, the availability of calibrated instruments and traceability of past operating procedures remains a major difficulty in homogenizing data sets to derive long-term trends (Ogren, 2011; Wiedensohler et al., 2012; Anderson and Ogren, 1998).

As a consequence, very few studies have addressed temporal changes of aerosol variables directly related to climate forcing using ground-based, in-situ aerosol measurements, namely scattering (σ_{sp}) and absorption (σ_{ap}) coefficients (and the derived quantities single scattering albedo, backscatter fraction (b), Ångström exponent ($å$)), number concentration (N), and size distribution. The issue of long-term trends in aerosol optical parameters has been the focus of only few publications. Depending on their focus, these papers typically describe either trends in one or more aerosol parameters for a single site/region (e.g. Collaud Coen et al., 2007; Bodhaine et al., 1993; Hirdman et al., 2010) or look at trends in a single parameter for a small group of sites (e.g. Sharma et al., 2006).

In this study, an analysis of in-situ aerosol optical property trends is performed within the framework of the WMO-GAW program, using quality-controlled information provided by the NOAA-affiliated monitoring network, the EMEP and EUSAAR/ACTRIS EU-based Research Infrastructure, and the US IMPROVE network, to provide indications of long-term changes in several climate-relevant aerosol variables. Analysis of long-term trends for N is dealt with in the companion paper (Asmi et al., 2013). This trend analysis is intended to answer the following questions:

1. Can any trends (positive or negative) in aerosol optical properties be detected and how do they differ as a function of length of data series (10 and 15 yr)?

2. Are there regional similarities or differences in the observed trends? Likewise, are there seasonal similarities or differences in the trends?

3. How do the observed optical property trends compare with trends in other aerosol properties reported in the literature?

The results presented here provide previously unavailable spatial and temporal coverage of aerosol variability in a changing climate. This kind of trend analysis may provide important perspectives on adverse climate side effects of air pollution control policies (e.g. Leibensperger et al., 2012) in the past and in the future.

2 Experimental

2.1 Measurement sites

The analysis presented here utilizes in-situ aerosol optical data from 24 observatories shown in Fig. 1 with site information listed in Table 1. The global network of long-term aerosol optical measurements is concentrated in the northern hemisphere, with 5 sites in Europe, 17 sites in North America, and only two sites in the Southern Hemisphere. Stations included in the study are all regional or global GAW (http://gaw.empa.ch/gawsis/) or IMPROVE (http://vista.cira.colostate.edu/improve/) sites located in rural/remote areas

and are expected to have large-scale spatial representativeness (see Henne et al. (2010) and Asmi et al. (2011) for the European sites), but the sparse coverage over most of the globe precludes calculation of global-average trends. Sites were chosen based on the following criteria: (a) availability of long-term (if possible > 10 yr, although three sites with 8–9 yr of data have also been included to improve spatial coverage) continuous measurements without ruptures in the aerosol light scattering and/or absorption measurement; (b) submission of quality-assured data to the WMO World Data Center for Aerosols; (c) responsiveness of site operators to questions concerning data quality and homogeneity. They are representative of rural continental, mountain, desert, marine, Arctic and Antarctic environments (Table 1) with only one station (PAZ) situated in a suburban environment. Some additional information about each of the sites included in this study is provided in the Supplement tied to this paper. Note: where there is a difference, we use the site ID tag in the GAWSIS database rather than the local/network site acronym or identifier.

2.2 Measurements, instruments and access to data

The data used here consist of hourly-averaged, quality-checked, light scattering and light absorption measurements. The data were collected as part of national contributions to the GAW aerosol programme (www.wmo.int/gaw/), as well as through the IMPROVE programme. The GAW aerosol data are archived at and available from the World Data Centre for Aerosol (WDCA, http://www.gaw-wdca.org) located at the Norwegian Institute for Air Research (NILU). The WDCA data are hosted in the EMEP database EBAS (http://ebas.nilu.no), an infrastructure shared with other frameworks targeting atmospheric aerosol properties, such as the European Aerosols, Clouds, and Trace gases Research InfraStructure Network (ACTRIS). The IMPROVE data are available from the IMPROVE website (http://vista.cira.colostate.edu/improve/Data/data.htm), and, with some delay, from the WDCA.

Table 1 describes the relevant instruments operated at each site and further instrument details are listed in Table 2. In all cases, light scattering was measured by integrating nephelometers and, for multi-wavelength instruments, at least one channel measured at a green wavelength (~ 550 nm) which is the wavelength for which scattering trends are reported. Light absorption was measured at various wavelengths by several filter-based instruments (i.e. particle soot absorption photometer (PSAP) and aethalometer (AE)); here, PSAP trends are reported at 550 nm, whereas the AE data at $\lambda = 840$–880 nm were usually used to determine trends (Table 2).

In addition to σ_{sp} and σ_{ap} trends, the following two parameters are evaluated for sites where nephelometers with multi-wavelength and backscatter capabilities (i.e. TSI nephelometers) were deployed (see Table 1):

1. scattering Ångström exponent, $\mathring{a} = -\ln(\sigma_{sp,1}/\sigma_{sp,2})/\ln(\lambda_1/\lambda_2)$
2. backscatter fraction, $b = \sigma_{bsp}/\sigma_{sp}$

where $\sigma_{sp,i}$ is the scattering coefficient at wavelength i, λ_i is the wavelength i and σ_{bsp} is the hemispheric backscattering coefficient. The single scattering albedo (ω_o) is another aerosol property that can be calculated using σ_{sp} and σ_{ap}; however we did not evaluate trends in ω_o because the absolute values of σ_{ap} were not determined for stations with AEs (no correction was made for the multiple scattering artifact for most AEs) so that the impact of σ_{ap} on ω_o trends would be biased. We were also unable to look at trends in absorption Ångström exponent due to the relatively short length of the available spectral absorption data sets, installation of multi-wavelength absorption instruments having being a relatively recent occurrence (within the last 5–6 yr) at most sites.

2.3 Data consistency

To determine long-term trends, internal data consistency for the individual stations is critical, but some latitude in data processing amongst stations was deemed acceptable. Specifically, some of the latitude allowed included whether the data sets had the same corrections applied; how the sites dealt with sample RH and very low aerosol amounts; and inlet size cuts. Table 1 has columns indicating information about size cuts, corrections, and RH conditions at the various sites. Below, general instrument conditions and corrections are briefly discussed.

One important factor affecting all aerosol measurements is the relative humidity (RH) at which the measurements are made. For σ_{sp}, measurements at controlled RH enable minimization of the confounding effects of aerosol hygroscopic growth and increases in the amount of scattering aerosol (Nessler et al., 2005a; Fierz-Schmidhauser et al., 2010). The disadvantage of making measurements at low RH is that aerosol hygroscopic properties must be measured or assumed in order to adjust the aerosol optical properties to ambient conditions. Within the GAW program, recommendations have been given to measure σ_{sp} at low humidities (see Table 1 for station RH statistics). With the exception of the IMPROVE and FKL nephelometers, the instruments are typically operated at RH $< 50\,\%$ or, in the case of PAL station, the data were provided screened so that only low RH measurements (RH $< 40\,\%$) were available, leading to preferential measurement of dry air masses. In contrast, the IMPROVE nephelometers measure at near ambient conditions (Malm et al., 1996). The mission of the IMPROVE network is to monitor visibility in protected environments (e.g. national parks), thus their operating conditions were chosen to reflect that visibility is a strong function of relative humidity. Several studies (e.g. Sisler and Malm, 1994; Malm et al., 2000; Day and Malm, 2001; Hand and Malm, 2007) have utilized the co-located aerosol chemistry measurements

Table 1. List of observatories included in this study, arranged alphabetically (Data range years are inclusive).

Station	Lat Long Elev (m) a.s.l.	Inst Scat[1] Abs[2]	Size cut (μm)	Data range Years scat data Years abs data	Corrections	Type[3]	Sample RH 5th, 50th, 95th percentile
ACA	44.38° N	O	–	1993–2010		Ma	40, 76, 100
Acadia NP[5],	68.26° W	–		–			
Maine, USA	157						
BBE	29.30° N	O	–	1998–2010		D	11, 40, 85
Big Bend NP,	103.18° W	–		–			
Texas, USA	1066						
BND	40.05° N	T	7	1994–2010	STP, A&O	RC	5, 20, 46
Bondville,	88.37° W	P		1996–2010	B1999,		
Illinois, USA	230				O2010[4]		
BRW	71.32° N	T	7	1998–2010	STP, A&O	A	0, 7, 22
Barrow,	156.6° W	P		1998–2010	B1999,		
Alaska, USA	11				O2010[4]		
FKL	35.34° N	R	Whole,	2001–2010		Ma	29, 64, 90
Finokalia,	25.67° E	AE22	then	2003–2010			
Greece	150		10				
GSM	35.63° N	O	–	1993–2010		RC	37, 74, 100
Great Smoky Mountain NP,	83.94° W	–		–			
Tennessee, USA	810						
HGC	35.97° N	O	–	1997–2010		D	15, 46, 94
Grand Canyon NP,	111.98° W	–		–			
Arizona, USA	2267						
HPB	47.80° N	T	Whole,	2002–2010	A&O	Mt	8, 21, 40
Hohenpeissenberg,	11.01° E	AE10	then	1995–2010			
Germany	985		10				
IBB	34.34° N	O	–	2001–2010		D	10, 29, 87
Ike's Backbone,	111.68° W	–		–			
Arizona, USA	1297						
JFJ	46.55° N	T	Whole	1995–2010	A&O	Mt	0, 7, 16
Jungfraujoch,	7.99° E	AE31		2001–2010	Collaud Coen		
Switzerland	3580				et al. (2010)		
MCN	37.13° N	O	–	1993–2010		RC	39, 78, 100
Mammoth Caves NP,	86.15° W	–		–			
Kentucky, USA	235						
MHD	53.33° N	T	Whole[6]	2001–2010		Ma	22, 34, 49
Mace Head,	9.90° W	AE9		2001–2010			
Ireland	5	and AE16					
MLO	19.54° N	T	10	2000–2010	STP, A&O	Mt	0, 6, 18
Mauna Loa,	155.58° W	P		2000–2010	B1999,		
USA	3400				O2010[4]		
MRN	46.76° N	O	–	1993–2010		RC	49, 92, 100
Mt. Rainier NP,	122.12° W	–		–			
Washington, USA	439						
MZW	40.54° N	O	–	1994–2009		Mt	27, 71, 100
Mt. Zirkel Wilderness,	106.68° W	–		–			
Colorado, USA	3243						
NMY	70.665° S	T	7–10	2001–2010	A&O	A	not available
Neumayer,	8.27° W	AE10		1999–2010			
Antarctica	42						
PAL	67.97° N	T	variable[7]	2000–2010	STP, A&O	RC	4, 14, 33
Pallas,	24.12° E	–					
Finland	560						
PAZ	33.50° N	O	–	2001–2009		D	10, 33, 80
Phoenix,	112.10° W	–		–			
Arizona, USA	372						

Table 1. Continued.

Station	Lat Long Elev (m) a.s.l.	Inst Scat[1] Abs[2]	Size cut (μm)	Data range Years scat data Years abs data	Corrections	Type[3]	Sample RH 5th, 50th, 95th percentile
SCN Sycamore Canyon, Arizona, USA	35.14° N 111.97° W 2046	O –	–	1998–2010 –		D/U	13, 51, 99
SGP Southern Great Plains, Oklahoma, USA	36.61° N 97.49° W 315	T P	7	1997–2010	STP, A&O B1999, O2010[4]	RC	6, 23, 52
SHN Shenandoah NP Virginia, USA	38.52° N 78.43° W 1079	O –	–	1996–2010 –		RC	36, 76, 100
SIA Sierra Ancha, Arizona, USA	34.09° N 110.94° W 1600	O –	–	2000–2010 –		D	11, 40, 94
SPO South Pole, Antarctica	89.98° S 24.8° W 2410	T –	Whole air	2003–2010 –	STP, A&O B1999[4]	A	0, 0, 0
THD Trinidad Head, California, USA	41.05° N 124.15° W 107	T P	7	2002–2010 2002–2010	STP, A&O B1999, O2010[4]	Ma	19, 30, 40

[1] More details in Table 2: T = TSI nephelometer, O = Optec nephelometer, R = Radiance Research nephelometer; [2] More details in Table 2: A = Aethalometer, P = 1-wavelength or 3-wavelength PSAP (all stations with PSAP upgraded from 1-wave to 3-wavelength version - see station appendix for details); [3] Station categories are; A = Arctic/Antarctic, D = Desert, Ma = Marine, Mt = Mountain, RC = Rural Continental, U = Urban/sub-urban; [4] STP = standard temperature (T = 273.15 K) and pressure, A&O = Anderson and Ogren (1998), B1999 = Bond et al. (1999) O2010 = Ogren (2010); [5] NP = National Park; [6] strong function of wind speed; [7] see station description in the Supplement.

Table 2. Measurement description.

Scattering Instrument, Model number	Scattering wavelengths (nm)[1]	Corrections	Manufacturer Info
TSI total/backscatter nephelometer, 3563	450, 550, 700	Anderson and Ogren (1998)	TSI, Inc. St. Paul, MN USA
Optec open-air nephelometer, NGN-2	550	none applied	Optec, Inc. Lowell, MI USA
Radiance Research nephelometer, M903	532	none applied	Radiance Research Seattle, WA, USA
Absorption Instrument, Model number	**Absorption wavelengths (nm)[1]**	**Corrections**	**Manufacturer Info**
Aethalometer AE9, AE10, AE16: white light	broadband centered at 840 nm[2]		Magee Scientific, Berkeley, CA USA
Aethalometer AE22: 2 wavelengths	370 and 880 nm[2, 3]		
Aethalometer AE31: 7 wavelength	370,470,520,590,660,880,950 nm[4]	Collaud Coen et al. (2010)	
PSAP – 1-wavelength	565[5]	Bond et al. (1999)	Radiance Research,
PSAP – 3-wavelength	467, 530, 660[5]	Ogren (2010)	Seattle, WA USA

[1] Reported by manufacturer; [2] the trend analysis were performed on the BC concentration reported by the manufacturer; [3] the 370 nm wavelength was used due to too noisy data at 880 nm; [4] the 880 nm wavelength was used to be the closest to white light sources; [5] in this work we use PSAP data adjusted to 550 nm, based on Bond et al. (1999) for 1-wavelength instrument or Ogren (2010) for 3-wavelength.

or additional low RH nephelometer measurements at IMPROVE sites to understand the hygroscopic nature of that aerosol and to adjust the measured scattering to "dry" conditions. Here, however, we analyze the IMPROVE scattering measurements at the measurement conditions, with a restriction of the σ_{sp} to values lower than 500 Mm^{-1} for stations in the eastern USA (ACA, GSM, MCN and SHN) and lower than 100 Mm^{-1} for stations in the western USA to minimize the influence of rain, fog, snow and ice. For the IMPROVE and FKL sites, the trends in RH and in measurements made during dry conditions by limiting the data set to RH < 50 % are also estimated and discussed. PSAPs are also sensitive to RH (e.g. Anderson et al., 2003), whereas AEs are much less affected by the aerosol hygroscopic growth (Nessler et al.,

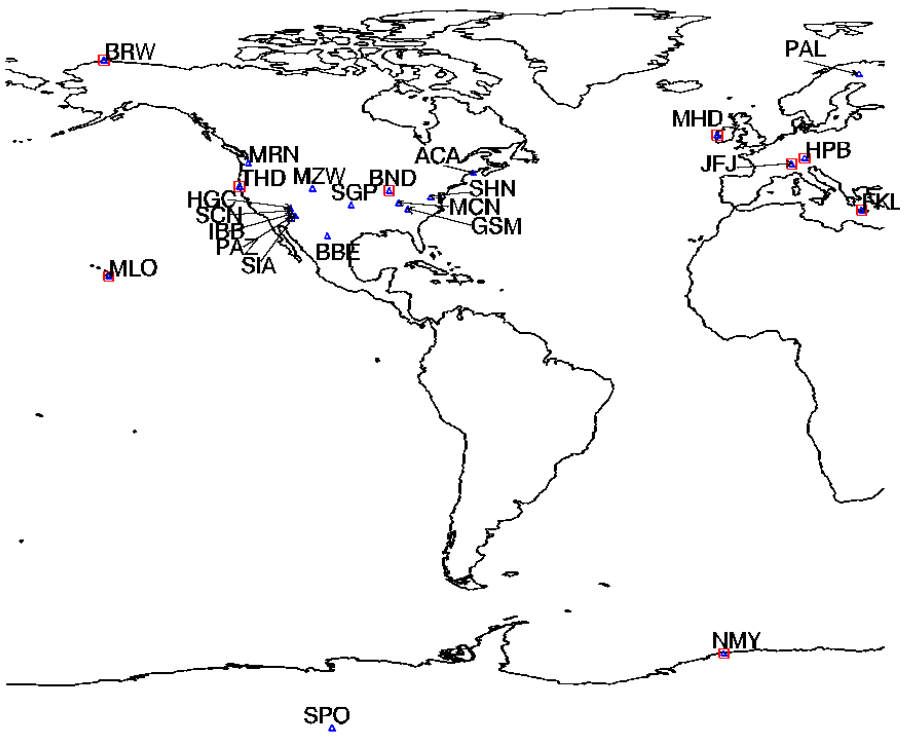

Fig. 1. Map of sites; blue triangles indicate sites with scattering data used in this paper, red squares indicate sites with absorption data used in this paper.

2005b). Almost all the sites included here that measured absorption implemented RH control on their sample air stream which would minimize the effect of RH on the absorption data. FKL installed RH control only in 2010 but show that it induced no difference in the AE absorption measurement. Unfortunately the 14 yr absorption record at SGP was influenced by high frequency humidity changes due to air conditioning cycling and those data are therefore not included in this study.

Another factor, aside from RH, that can affect σ_{sp} and to a lesser extent σ_{ap} is particle size. Size effects can happen in several ways such as changes in inlet properties or length of pipes. Inlet changes are documented in the station descriptions in Supplement. Only datasets for which inlet changes reported by data providers did not appear to have a noticeable effect on the measured aerosol optical properties have been used. When the inlet changes induced break points in the analyzed parameters, only data from the most recent inlet were utilized in the analysis.

Another, less direct, effect of particle size on scattering is related to non-idealities in the nephelometer measuring over a truncated angular range (Müller et al., 2009). All TSI nephelometer scattering data sets included here are adjusted for instrument non-idealities using the Anderson and Ogren (1998) correction. The Radiance Research nephelometer at FKL has similar truncation characteristics to the TSI nephelometer (Müller et al., 2009), however no truncation adjustment was applied to the FKL scattering data. The Optec nephelometer measures over a wider angular range (5–175°) (Molenar, 1997) than the TSI and Radiance Research nephelometers but like the Radiance Reseach measurements, the scattering has not been corrected for truncation. The Optec nephelometers measure at ambient conditions with no size cut (they are open air instruments) so they can sample very large particles due to both hygroscopicity and/or the presence of precipitation, fog, dust, pollen, etc. Thus, for times when enhanced amounts of large diameter ($D_p > 1$ µm) particles are present, the measured scattering will be lower than true scattering by a substantial amount because the truncation correction increases with particle size (Anderson and Ogren, 1998; Molenar et al., 1997).

The instrumentation to measure σ_{ap} has undergone significant development during the last 15 yr, leading to instrument changes/upgrades in the field, which, at some sites, introduced irreducible break points in long-term data sets. The two methods for measuring absorption coefficient used in this study (PSAP, Radiance Research, Seattle, USA and Aethalometer, Magee Scientific, Berkeley, USA) are both filter-based instruments in which changes in light transmission through the filter, due to particle deposition on the filter, are attributed to absorbing aerosol. In general, the filter-based method applied to measure σ_{ap} suffers from several instrumental artifacts that can potentially lead to negative values in the case of very low amounts of absorbing aerosol and

generally to over-prediction of absorbing aerosol due to multiple scattering in the filter matrix and to the aerosol type (e.g. Bond et al., 1999; Müller et al., 2011; Collaud Coen et al., 2010).

The five PSAP data sets in this study are from instruments in the NOAA collaborative network. The PSAP data are processed using Bond et al. (1999) to account for issues like spot size and scattering artifacts. Over the period of time reported here, all PSAPs were upgraded from the 1-wavelength to 3-wavelength version; Ogren (2010) adjustments to the Bond algorithm to account for wavelength changes were applied following the instrument upgrade. All PSAP upgrades occurred in 2005 and 2006; the date of the PSAP changes for each NOAA collaborative site is provided in the individual station descriptions in the appendix. The PSAP upgrades did not induce marked break points in the absorption measurement reported at 550 nm, thus the entire data set for each site was used.

Data from several models of aethalometer were used including white light and multi-wavelength light sources (see Tables 1 and 2). Multiple corrections have been published to address known artifacts of the aethalometer measurement (e.g. Collaud Coen et al., 2010). For most of the aethalometer data sets, only the manufacturer's suggested corrections (Weingartner et al., 2003) were applied and the trends were calculated on the equivalent black carbon (BC) concentrations. At JFJ, the correction by Collaud Coen et al. (2010) was applied, and trends were calculated on light absorption. It was, however, verified that application of the Collaud Coen correction did not influence the JFJ absorption trend.

The differences in instrumentation, measurement conditions, and post-processing data treatment do not allow the absolute values of σ_{sp} and σ_{ap} for all sites to be compared; however, because there was consistency of data treatment for individual sites, the trends can be compared.

2.4 Discontinuities in the data and homogenization of data sets

Long-term climate analyses require homogeneous time series to be accurate. A homogeneous climate time series is defined as one where variations are caused only by variations in weather and climate (Conrad and Pollak, 1950) and in emissions of aerosol particles and their precursor gases. Unfortunately, most long-term climatological time series have been affected by a number of non-climatic factors called inhomogeneities (e.g. relocations, instrument upgrades, inlet changes, nearby pollution sources, etc.) that make these data unrepresentative of the actual climate variation occurring over time. The time at which an inhomogeneity occurs is called a break point. To detect break points, all the data sets used in this study were examined in a variety of ways, including visual inspection of linear and logarithmic plots, comparison of yearly cycles, investigation of both extreme and negative values, and inspection of the fit residues (see Sect. 2.5.4 and related figures) (see also companion paper, Asmi et al., 2013). In addition, the data owners responded to a questionnaire about potential break points, providing meta-data that could be used to confirm/dismiss possible break points or to accurately locate them. Where possible, the data were edited to remove the break points. Only data sets considered as homogeneous by the authors and the data owners were analyzed in this study. The data homogenization process provides us with our first finding – that a critical review of the data by others outside the measurement network is very important in improving the quality of the reported data.

The WDCA/EBAS data submission guidelines provide multiple options for data flagging (e.g. contamination due to local influence, contamination due to wind sector, data problem due to mechanical issues, etc.). However, these are only options and the individual data providers approach flagging differently based on how their site is operated and the complexity of their post-processing QC. Other sites may not include contaminated data; for example, some sites in the NOAA network identify a wind-sector angle for which the data may be contaminated due to a nearby source (e.g. the town of Barrow, for BRW or upslope flow conditions for MLO) and the data from the polluted sector are not included in the hourly averaged data submitted to WDCA/EBAS. Other sites may identify typical air masses as a function of wind direction (e.g. marine vs continental at MHD), but this information is not included in the data set submitted to WDCA and instead must be obtained from the data provider. There is some information about flagging criteria for each station included in the station description in the Supplement.

2.5 Trend analysis description

None of the aerosol parameters analyzed here are normally distributed. Most of the parameters have an approximately lognormal distribution or can sometimes consist of the sum of two lognormal distributions. We chose therefore to use two non-parametric tests, the seasonal Mann-Kendall (MK) test associated with the Sen's slope and the generalized least square trends with either autoregressive or block bootstrap confidence intervals (GLS/ARB), to detect s.s. trends and estimate their magnitude, and the least-mean square (LMS) fit applied to the data logarithms in order to have a further estimate of the trends. These methods are described below.

The MK method is the most appropriate test to use for optical properties because it can be applied regardless of missing values, statistical distribution and presence of negatives in the data set. Moreover a brief analysis showed that the MK method was the most sensitive to very small trends, since most of our datasets do not follow a normal distribution. The MK method is however very sensitive to autocorrelation in the data, and the pre-whitening procedure applied presents some limitations since the autocorrelation is not a pure autoregressive stationary (AR(1)) process. The GLS/ARB method was applied on the data for the optical

properties to include negative values; it is therefore less appropriate since the not-normal distribution was not accounted for. It is however able to correctly handle the data autocorrelation and noise non-idealities. While the LMS method applied to the logarithm of the data monthly medians correctly handles the data distribution, it is unable to account for negative values and, additionally, autocorrelation will remain in datasets with high seasonality.

In this analysis, there is no method that is completely satisfactory for answering all difficulties raised by the studied datasets. The MK method has been taken as the reference method since it seems to be the most sensitive to small trends and the slope determination does not suffer from any statistical restriction. For scattering and absorption coefficients, the LMS method working with monthly instead of daily values clearly seems to miss some trends. For b and $å$, the MK method detects fewer s.s. trends than found by the other 2 methods. This could be attributed to the distributions of these parameters being closer to the normal distribution than the scattering and absorption coefficients; it is well-known that MK sensitivity is lower than other statistical methods for normal distributions.

2.5.1 Seasonal Mann-Kendall test

The Mann-Kendall test is a non-parametric technique based on rank (Sirois, 1998; Gilbert, 1987), which is a particular application of Kendall's test for correlation commonly known as Kendall's tau. The MK test determines if a monotonic increasing or decreasing long-term trend exists. This method is particularly useful since missing values are allowed and the data do not need to conform to any particular distribution. It is now well understood that autocorrelation in the data can have a broad influence on the analysis leading to an overestimation of the statistical significance (Yue et al., 2002; Zhang and Zwiers, 2004) and that "pre-whitening" is the best method to eliminate the influence of AR(1) serial correlation on the Mann-Kendall test (Wang and Swail, 2001; Bayazit and Önöz, 2007). The pre-whitening method described by Wang and Swail (2001) consists of the following iterative process: (1) estimate the auto-correlation, (2) while the auto-correlation remains higher than 0.05, calculate the Sen's slope, (3) remove the linear trend using the Sen's slope, (4) remove the auto-correlation and (5) add the trend. This pre-whitening procedure was therefore applied to the data prior to the Mann-Kendall trend analysis. Hirsch et al. (1982) extend the Mann-Kendall test to take seasonality in the data into account as well as multiple observations for each season. They called this test the seasonal Mann-Kendall test. To test for either an upward or downward trend, a two-tailed test at the 95 % level of significance was applied. Because data sets were quite noisy at hourly frequency due to the very low aerosol concentration of some remote sites, the statistical significance of the MK method reported here was estimated from the daily medians and not from the hourly measurements.

2.5.2 Sen's slope estimator

If a linear trend exists, the true slope can also be estimated by a non-parametric procedure developed by Sen (1968), which is closely linked to the Mann-Kendall test. Sen's method is not greatly affected by outliers and can be computed when there are gaps in the data set. Sen's estimator of the slope is the median of individual slopes of all data pairs $x_i(t_i)$ and $x_j(t_j)$ with $j > i$. A 90 % confidence level was used to calculate the upper (UCL) and lower (LCL) confidence limits using the procedure described by Gilbert (1987). Due to a limitation in the allowed matrix dimension, Sen's slopes were not calculated using the hourly values directly, but rather using the median of 24 or 48 h values, depending on the data set size.

Figure 2 shows an example of the MK method for the ACA σ_{sp} (at 18 yr, ACA is one of the longest data sets in this study). The clear seasonality of the trend can be observed in Fig. 2a (see discussion section for more details), as well as the marked increase of the size of the confidence limits (blue lines) with decreasing length of the data set. Due to the fact that the confidence limits are calculated from the Sen's slope estimator but the significance of the trends is determined by the MK method, the trends can be s.s. even if the confidence limits cross zero. Figure 2b shows all the 5 yr trends that can be calculated for the ACA data set. Several observations support the decision not to analyse data sets shorter than 8 yr: (1) both positive and negative s.s. trends are observed; (2) the slopes for the shorter term trends are much larger than the slopes for the long-term trends, ranging from -60 to $+20$ % yr^{-1}, compared to -7 to $+1$ % yr^{-1} for the long-term trends; and (3) the confidence intervals are consequently much greater for short time periods than those found for the long-term trends.

2.5.3 Bootstrapping method associated with Monte-Carlo

The Generalized Least Squares (GLS) method was also used to evaluate the trends. The method is based on the minimization of the least square errors similar to ordinary least squares fitting (including similar sensitivity to outliers), but taking into account the autocorrelation in the covariance matrix. The GLS method was combined with an autoregressive bootstrap (ARB) algorithm to evaluate the potential differences in the GLS trends arising from the noise terms. This ARB methodology was used to produce 1000 realizations of the original time series, with randomized noise terms, and the resulting set of trends was used to get 5th to 95th percentile confidence intervals (ARB CIs) of the GLS trends. If the ARB CIs did not include a zero trend, we considered the GLS trend to be s.s. The GLS and ARB methodologies were adapted from

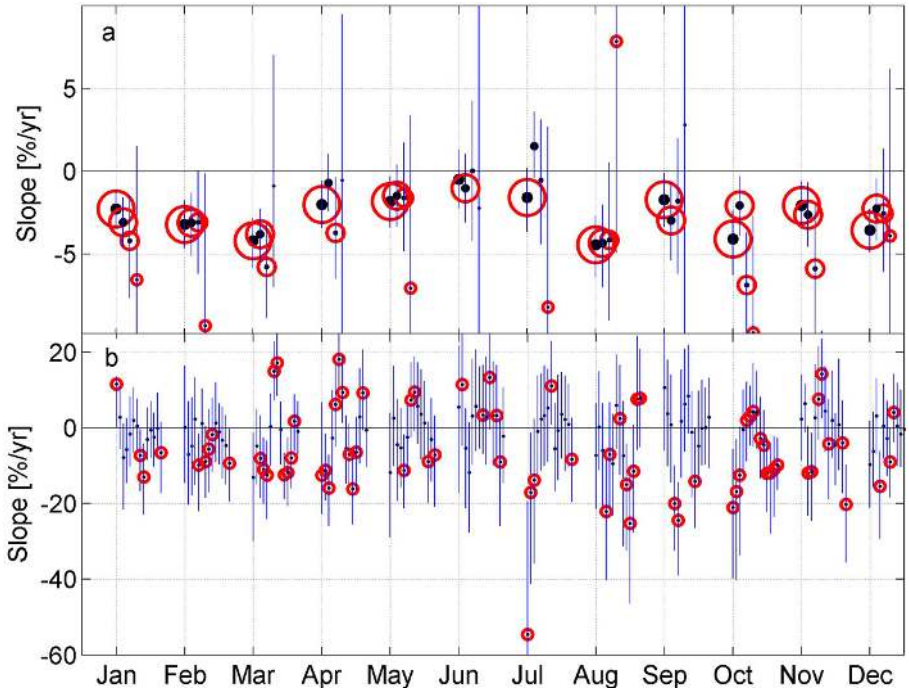

Fig. 2. Seasonal MK trend analysis of the ACA scattering coefficient: **(a)** trends of the entire dataset (18 yr), of the last 15, 10 and 5 yr, the size of the points and of the circles corresponding to the analyzed length of time, **(b)** MK trend analysis of all possible 5 yr trends for the ACA dataset. Black points correspond to Sen's slopes, red circles to slopes that are statistically significant at the 95 % confidence levels, respectively. Blue lines correspond to the Sen's slope 90 % confidence limits.

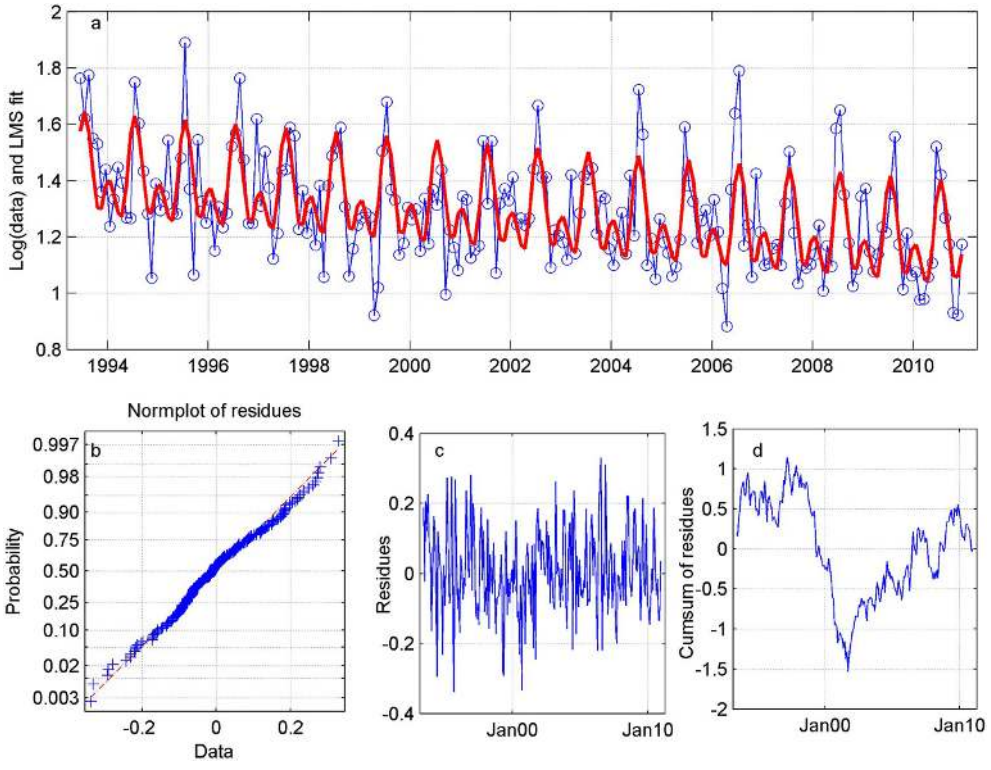

Fig. 3. LMS trend analysis of the ACA scattering coefficient: **(a)** logarithm of the data monthly medians in blue and LMS fit in red, **(b)** normal probability plot of the residues, **(c)** time series of the residues and **(d)** cumulative summation of the residues.

Mudelsee (2010) and applied to daily medians; more details of the application is in our companion paper (Asmi et al., 2013).

2.5.4 Least-mean squares fit

Following the Weatherhead procedure (Weatherhead et al., 1998, 2000), the trend is estimated by fitting the following frequently used statistical model for monthly data with an LMS approximation:

$$Y_t = m + C_t + \rho \cdot (t/12) + M_t, \quad t = 1 \ldots n, \tag{1}$$

where m is a constant term, C_t is a seasonal component, and ρ is the magnitude of the trend per year. The unexplained noise term M_t is modeled as an (AR(1)) process $M_t = \phi \cdot M_{t-1} + \epsilon$, where ϕ is the autocorrelation coefficient of the data noise. When the measured aerosol variables were approximately lognormally distributed, Y_t was taken as the logarithm of the monthly medians. We shall adopt the commonly used decision rule that a real trend is indicated at the 95 % confidence level when $|\rho/\sigma_\rho| > 2$, σ_ρ being the standard deviation of the slope. Figure 3 shows the LMS trend and statistics for the ACA σ_{sp}. The clear seasonality of σ_{sp} is visible as well as the decreasing trend. The normal probability plot of the log(data) (Fig. 3b) clearly shows that the data are approximately lognormally distributed while the plot of the residues (Fig. 3c) does not reveal any break points in the data set. The cumulative summation of the residues (Fig. 3d) clearly shows that 2000 and 2001 have lower summer maxima that are below the decreasing trend.

3 Results

Before presenting results, we provide a few definitions of the terms used through the rest of this paper. The term "significant" or "significance" should always be understood as "statistically significant at the 95 % confidence level". To obtain the relative trends in % yr^{-1}, the slope was divided by the median value of the entire data set. To allow comparison among the data sets covering different lengths of time, we chose to restrict the data sets' end point to 2010, since not all stations submitted 2011 data soon enough. The trend analyses were not only performed on the whole data set but also on the last 10 yr (2001–2010) and, if possible, on the last 15 yr (1996–2010).

3.1 Scattering coefficient trends

Long-term trend analysis of σ_{sp} has been performed on 24 data sets in Europe, North America and Antarctica. The large number of scattering data sets is due both to the inception of nephelometer measurements at IMPROVE network sites in the 1990's (10 of the 12 IMPROVE stations included here began nephelometer measurements in the 1990's) and also to the robust nature of nephelometers which allowed for good quality data sets with minimal break points. The detailed results of MK, GLS/ARB and LMS trend analyses are given in Table 3 while the overall picture is presented in Fig. 4.

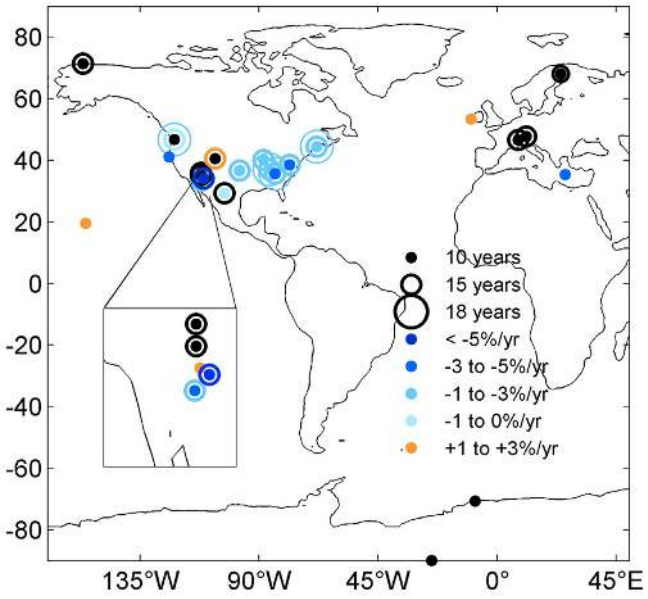

Fig. 4. MK trends results for the scattering coefficient. Black symbols correspond to stations with no significant trends. Blue and orange symbols correspond to statistically significant negative and positive trends, respectively, the magnitude of the trends (slope) being given by the colors as stipulated in the legend. The sizes of the circles are proportional to the length of the data sets; the trend for the whole period as well as the 10 yr (dots) and, if possible, 15 yr trends were calculated. The largest circles denote, therefore, the trend of the longest analyzed period.

The σ_{sp} s.s. trends are predominantly negative: 75 % of the s.s. 10 yr trends using the MK method are negative, and for the 15 yr trends 87 % are negative. Nearly half (42 %) of the stations did not have s.s. scattering trends for the 10 yr period, but only 1 station out of 9 (11 %) did not have a s.s. trend when the 15 yr period was considered. Results obtained with the MK method were confirmed using the GLS/ARB method. The MK slopes ranged between -3 and -60 % 10 yr^{-1} and GLS/ARB slopes between -1 and -85 % 10 yr^{-1} and LMS changes for 2001–2010 period ranged between -6 to -20 %. The analysis of long-term scattering measurements from two mountaintop sites in Europe, two desert stations in Arizona and the Arctic site revealed no s.s. trends. Using the MK method, s.s. positive trends in scattering are observed at four sites – a marine site in Europe, two desert locations in the southwest US and a free troposphere mountain site in the Pacific Ocean. No s.s. trends in light scattering were observed for the two southern hemisphere sites in this study. The main results are as follows:

Table 3. Significance and slope of the trends of the scattering coefficient calculated with the MK, GLS/ARB and LMS methods for the entire measured periods (all), and for 15 yr and 10 yr when possible. The statistically significant trends at 95 % confidence level are highlighted in bold. Only the significance of the LMS fits is mentioned for the entire measured periods, since the LMS results deal with the data logarithm; for the 10 yr period, the changes in % over the 2001–2010 period were calculated from the LMS slopes in order to allow comparison with the other 10 yr slopes.

Station	Units	MK			GLS/ARB			LMS	
		All	15 yr	10 yr	All	15 yr	10 yr	Significance, all	Change 2001–2010 (%)
US (apart from Arizona)									
ACA	$Mm^{-1}\,10\,yr^{-1}$	**−4.2**	**−3.6**	**−4.5**	**−11.7**	**−9.1**	**−10.1**	**Negative**	
	$\%\,10\,yr^{-1}$	**−27.4**	**−24.7**	**−31.9**	**−76.1**	**−59.2**	**−65.7**		**−12.37**
BBE	$Mm^{-1}\,10\,yr^{-1}$	−1.6		**−0.7**	**−2.3**		**−4.0**	No trend	
	$\%\,10\,yr^{-1}$	−10.8		**−4.7**	**−15.5**		**−27.5**	**Negative** for 10 yr	**−6.50**
BND	$Mm^{-1}\,10\,yr^{-1}$	**−17.2**	**−17.2**	**−11.3**	**−11.5**	**−11.5**	**−10.0**	**Negative**	
	$\%\,10\,yr^{-1}$	**−27.6**	**−27.6**	**−19.4**	**−18.4**	**−18.4**	**−17.2**		**−8.03**
GSM	$Mm^{-1}\,10\,yr^{-1}$	**−11.0**	**−11.4**	**−20.6**	**−21.1**	**−21.3**	**−33.9**	**Negative**	
	$\%\,10\,yr^{-1}$	**−23.9**	**−25.1**	**−47.2**	**−46.0**	**−47.1**	**−77.7**		**−8.36**
MCN	$Mm^{-1}\,10\,yr^{-1}$	**−11.0**	**−11.4**	**−20.6**	**−14.6**	**−20.0**	**−29.2**	No trend	
	$\%\,10\,yr^{-1}$	**−23.9**	**−25.1**	**−47.2**	**−31.8**	**−44.2**	**−66.9**		−2.07
MLO	$Mm^{-1}\,10\,yr^{-1}$	**0.3**		**0.3**	**1.4**		**1.4**	**Positive**	
	$\%\,10\,yr^{-1}$	**27.4**		**27.4**	**148.9**		**148.9**		**11.18**
MRN	$Mm^{-1}\,10\,yr^{-1}$	**−3.5**	**−1.5**	3.0	**−4.0**	**−2.3**	−1.0	No trend	
	$\%\,10\,yr^{-1}$	**−12.9**	**−5.5**	11.3	**−14.7**	**−8.6**	−3.8		4.14
MZW	$Mm^{-1}\,10\,yr^{-1}$	**3.1**	**2.6**	0.5	**4.8**	**3.4**	**3.9**	**Positive**	
	$\%\,10\,yr^{-1}$	**27.2**	**21.9**	4.0	**41.7**	**28.5**	**31.0**		**21.66**
SGP	$Mm^{-1}\,10\,yr^{-1}$	**−9.5**	**−9.5**	**−8.2**	**−8.9**	**−8.9**	**−9.8**	**Negative**	
	$\%\,10\,yr^{-1}$	**−26.3**	**−26.3**	**−20.2**	**−24.6**	**−24.6**	**−24.2**	(no trend for 10 yr)	−5.44
SHN	$Mm^{-1}\,10\,yr^{-1}$	**−10.4**	**−10.4**	**−15.3**	**−21.4**	**−21.4**	**−32.3**	No trend	
	$\%\,10\,yr^{-1}$	**−26.4**	**−26.4**	**−40.5**	**−54.6**	**−54.6**	**−85.3**		−4.04
THD	$Mm^{-1}\,10\,yr^{-1}$	**−0.65**			**−0.85**			**Negative**	
	$\%\,10\,yr^{-1}$	**−3.51**			**−4.59**				
Southwestern US (Arizona)									
HGC	$Mm^{-1}\,10\,yr^{-1}$	0.3		−0.8	0.25		−0.11	No trend	
	$\%\,10\,yr^{-1}$	2.9		−8.1	2.8		−1.2		−1.41
IBB	$Mm^{-1}\,10\,yr^{-1}$	**2.5**		**2.5**	1.5		1.5	**Positive**	
	$\%\,10\,yr^{-1}$	**22.6**		**22.6**	13.6		13.6		**11.47**
PAZ	$Mm^{-1}\,10\,yr^{-1}$	**−7.3**		**−9.6**	**−4.5**		**−5.2**	**Negative**	
	$\%\,10\,yr^{-1}$	**−26.5**		**−36.9**	**−16.3**		**−20.0**		**−9.86**
SCN	$Mm^{-1}\,10\,yr^{-1}$	−0.7		0.0	1.1		1.5	No trend	
	$\%\,10\,yr^{-1}$	−6.1		−0.3	9.2		12.8		1.58
SIA	$Mm^{-1}\,10\,yr^{-1}$	**−7.2**		**−6.5**	**−7.4**		**−7.4**	**Negative**	
	$\%\,10\,yr^{-1}$	**−68.4**		**−61.9**	**−70.7**		**−70.5**		**−20.42**
Europe									
FKL	$Mm^{-1}\,10\,yr^{-1}$	**−22.0**			**−12.8**			**Negative**	
	$\%\,10\,yr^{-1}$	**−50.6**			**−29.4**				
HPB	$Mm^{-1}\,10\,yr^{-1}$	−0.02		3.7	**4.9**		1.6	No trend	
	$\%\,10\,yr^{-1}$	−0.1		17.2	**23.4**		7.4		−1.15
JFJ	$Mm^{-1}\,10\,yr^{-1}$	0.13	0.1	−0.39	−0.4	−0.02	**−1.2**	No trend	
	$\%\,10\,yr^{-1}$	5.0	3.6	−12.0	−14.7	−0.7	**−37.0**		−11.45
MHD	$Mm^{-1}\,10\,yr^{-1}$	**4.3**		**4.3**	2.5		2.5	No trend	
	$\%\,10\,yr^{-1}$	**26.5**		**26.5**	15.4		15.4		11.11
PAL	$Mm^{-1}\,10\,yr^{-1}$	−1.8		−0.4	−2.2		−2.2	No trend	
	$\%\,10\,yr^{-1}$	−38.8		−9.0	−47.9		−48.4		−8.22
Arctic and Antarctic									
BRW	$Mm^{-1}\,10\,yr^{-1}$	0.8		1.4	1.10		1.90	No trend	
	$\%\,10\,yr^{-1}$	14.5		24.0	19.5		32.5		15.65
NMY	$Mm^{-1}\,10\,yr^{-1}$	0.4		0.4	0.4		0.4	No trend	
	$\%\,10\,yr^{-1}$	24.7		24.7	24.7		24.7		−9.24
SPO	$Mm^{-1}\,10\,yr^{-1}$	0.01			0.02			No trend	
	$\%\,10\,yr^{-1}$	1.14			3.32				

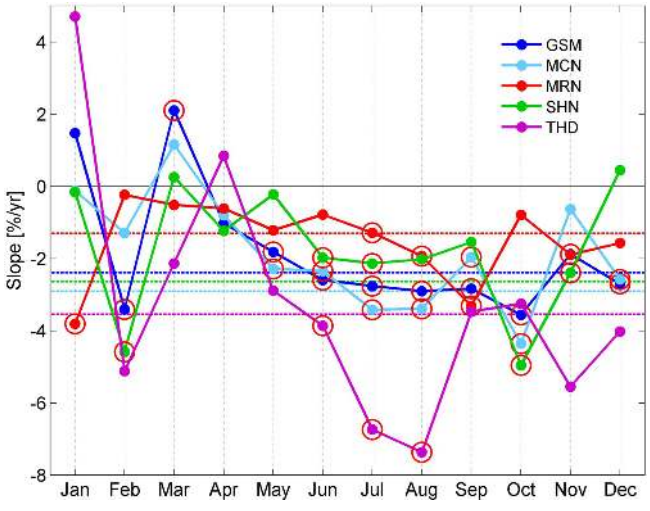

Fig. 5. Seasonal Mann-Kendall trend analysis (red circles correspond to 90 % confidence levels) associated with Sen's slopes (colored dots) for the scattering coefficients of eastern and northwestern stations. The dotted lines correspond to the annual trend.

- Over the continental US, trends are generally negative (of the order of -2 to $-3\,\%\,\mathrm{yr}^{-1}$) and s.s. regardless of the method used for derivation. This is the case for all stations located east of the Rocky Mountains (ACA, BND, GSM, MCN, SGP, SHN) and for the 2 stations located in the northwestern US (MRN and THD) when the entire period of measurement was considered. However, it should be noted that no s.s. scattering trend at MRN is found when just the last 10 yr are analyzed. The calculated trends in scattering for the five sites located in the arid state of Arizona (HGC, SCN, IBB, PAZ and SIA) are not consistent with each other. Decreasing trends were found for the two sites in southern Arizona (SIA and PAZ) for all methods. There was no s.s. trend in scattering for either of the high altitude sites in northern Arizona (HGC at 2267 m a.s.l. and SCN at 2046 m a.s.l.). Significant positive trends are derived for two sites, one (MZW) located at high altitude (3242 m a.s.l.), the other in the central Arizona desert (IBB). For the IBB site, a s.s. increasing trend in scattering was found, but only with the MK and LMS methods. We can therefore conclude that, except for specific stations, there is a very general and robust decrease in aerosol σ_{sp} observed over the last 10 to 15 yr, detectable despite the high natural variability of the atmospheric aerosol.

- Few s.s. trends were observed for the five European sites. FKL is the only Europe station for which a s.s. decreasing trend in σ_{sp} was found. In contrast, the analysis of long-term scattering measurements from two mountaintop sites (JFJ and HBP), and one site in a high latitude boreal region (PAL) revealed no s.s. trends. Finally, a s.s. positive change in scattering is observed at the coastal Atlantic site (MHD) when derived with the MK method (a positive but not s.s. trend is found with GLS/ARB and LMS). Note that the MHD data set was not flagged to separate the marine and continental influences, thus it is difficult to ascribe the MHD trend to changes in sources.

- We found no s.s. scattering trends for the Arctic site (BRW) or Antarctic sites (NMY, SPO), while a positive trend was derived for the free troposphere mountain site in the Pacific Ocean (MLO) regardless of the used statistical method.

- A clear seasonality was found for the eastern US stations of GSM, MCN, SHN and the western US stations of MRN and THD (Fig. 5). In general, the slopes were less significant from January to March, the trends increase in the spring, and there were high negative slopes from June to September. The maximum negative slope was found in October for the three eastern stations. The large seasonal slopes observed at THD are attributed to the fact that it was a relatively short data set (only 9 yr). Seasonality in the trends was also observed for ACA, MLO and several of the Arizona desert sites (PAZ, SIA and IBB) – this is discussed more in Sects. 4.2 and 4.3. There was no obvious seasonality observed for many sites (BND, SGP and MZW). However, no clear seasonality in scattering trends was observed for either the European or polar sites.

A trend in the atmospheric water vapour content (e.g. due to drought conditions) could change the aerosol size distribution and thus could influence trends in σ_{sp}. As mentioned in Sect. 2, the IMPROVE and FKL stations measure scattering at near ambient conditions, so that the RH of the measured air is typically significantly higher than for the GAW stations. The RH trends have therefore been estimated for FKL and all IMPROVE stations using an LMS method involving monthly means, since RH is normally distributed. The LMS trends are given in Table 4. Only three stations (ACA, FKL and PAZ) had s.s. negative RH trends (-0.22, -1.73 and $-1.3\,\%\,\mathrm{yr}^{-1}$, respectively) which could explain the observed negative scattering trends for these three sites. However, when the analysis is restricted to RH $< 50\,\%$ (corresponding to 13, 25 and 75 % of the ACA, FKL and PAZ datasets, respectively) the MK trends remain s.s. and negative, but with smaller slopes of $-1.25\,\%\,\mathrm{yr}^{-1}$ and $-1.61\,\%\,\mathrm{yr}^{-1}$ for ACA and PAZ, respectively, and a larger slope of $-8.8\,\%\,\mathrm{yr}^{-1}$ for FKL. In the case of FKL, dry air masses most of the time correspond to dust intrusion, so that the larger reported trend for RH $< 50\,\%$ can be primarily attributed to mineral dust influence. Note: we also looked at scattering trends when RH $< 50\,\%$ for the RH-controlled stations, but adding this constraint had little effect on the outcome as RH conditions were typically $< 50\,\%$.

Table 4. LMS trend of the RH percentage measured by the IMPROVE site Optec nephelometers. The trend are statistically significant at 95 % confidence limit if $\rho/\sigma_\rho > 2.00$ and at 90 % confidence limit if $1.67 < \rho/\sigma_\rho < 2.00$.

Stations	LMS slope (unit yr^{-1})	Slope (% yr^{-1})	ρ/σ_ρ
ACA	**−0.22**	**−0.16**	**2.2**
BBE	0.55	0.24	0.83
FKL	**−1.73**	**−1.08**	**2.79**
GSM	−0.23	−0.16	1.47
HCG	−0.23	−0.11	0.44
IBB	0.34	0.12	0.26
MCN	−0.14	−0.11	0.94
MRN	−0.05	−0.044	0.56
MZW	−0.12	−0.08	0.50
PAZ	**−1.34**	**−0.49**	**2.23**
SCN	−0.17	−0.08	0.26
SHN	−0.14	−0.1	0.82
SIA	1.23	0.55	1.31

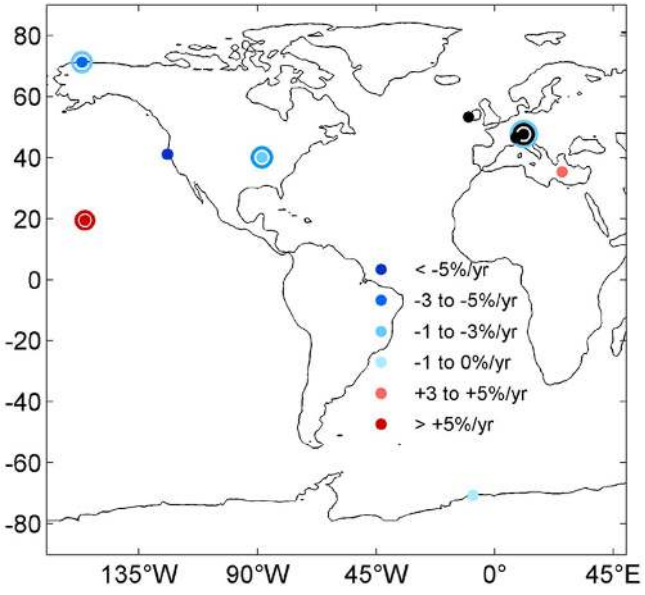

Fig. 6. Mann-Kendall trend results for the absorption coefficient. The symbols have the same meaning as in Fig. 4.

3.2 Absorption coefficient trends

The long-term trend analysis of aerosol absorption has been performed on nine datasets in Europe, North America and Antarctica (Fig. 6 and Table 5). Some of the absorption data sets used here include many negative values (30 % at NMY, 12 % at JFJ, 10 % at BRW and MLO) in the hourly data. These are very clean sites so the negatives are primarily the result of instrument noise at low aerosol loading. Due to the continuity of the measurements and the small number of stations with long-term absorption measurements, these sites were still included in the trend analysis. The main results are:

- In the continental US, the number of long-term absorption data sets (3) is significantly lower than the number of scattering data sets (17) due to the fact that IMPROVE stations do not monitor absorption but only elemental carbon (EC) as part of wider chemical analysis. Generally, the σ_{ap} trends are similar to σ_{sp} trends. Both BND and THD stations have s.s. negative trends with the BND absorption trend slope being quite similar to the station's σ_{sp} trend (-3.1 % yr^{-1}). In contrast the absorption trend at THD has a much larger negative slope (-13.0 % yr^{-1}) than was observed for σ_{sp} (-3.51 % yr^{-1}).

- In Europe, absorbing aerosol trends can be derived for 4 sites. No s.s. trends are observed for the two high altitude stations of JFJ and HPB for the last 10 yr; the full dataset at HPB has a s.s. negative trend of -1.6 % yr^{-1} over 16 yr. No s.s. trend in absorbing aerosol was observed for the marine station MHD regardless of analysis method. In contrast, the marine station FKL has a s.s. positive absorbing aerosol trend of 4.6 % yr^{-1} for the 8 yr of available data when it is evaluated with the MK method, however the trend is negative but not s.s. when the GLS/ARB method is used.

- The high altitude site of MLO has a s.s. positive trend in absorption (+8.44 % yr^{-1}), which is the same sign but larger magnitude than was observed for σ_{sp} (+2.74 % yr^{-1}).

- Both of the polar stations (BRW and NMY) have s.s. negative absorbing aerosol trends, although no trends were observed in scattering for either site. The analysis of NMY remains suspicious due to the high percentage of negative values observed.

- At BRW the absorption trend had a seasonal component – the winter maxima (January–February) of σ_{ap} clearly decreased over the measurement period, while the summer minima remained stable. THD presents the same seasonality for both σ_{ap} and σ_{sp} (Fig. 5). No clear seasonality in σ_{ap} was observed at any of the other sites.

3.3 Backscatter fraction and scattering Ångström exponent trends

Both b and $\mathring{a}$ are calculated using ratios of two nephelometer measurements (Eqs. 1–2). Stations in clean locations with very low aerosol σ_{sp} will have outliers in both b and $\mathring{a}$ values due to noise from taking the ratio of uncertain numbers. To reduce this problem, b and $\mathring{a}$ were calculated from the daily medians of σ_{sp}. Even with this approach, outliers still appeared in the calculated parameters and resulted in larger

Table 5. Significance and slope of the trends of the absorption coefficient; the color scheme and labels are similar to Table 3.

Station	Units	MK			GLS/ARB			LMS	
		All	15 yr	10 yr	All	15 yr	10 yr	Significance, all	Change 2001–2010 (%)
US									
BND	$Mm^{-1}\,10\,yr^{-1}$	**−0.8**	**−0.8**	**−0.5**	**−1.2**	**−1.2**	**−0.8**	No trend	
	$\%\,10\,yr^{-1}$	**−31.4**	**−31.4**	**−20.3**	**−47.1**	**−47.1**	**−32.5**		−6.02
MLO	$Mm^{-1}\,10\,yr^{-1}$	**0.1**		**0.1**	**0.18**		**0.18**	**Positive**	
	$\%\,10\,yr^{-1}$	**84.4**		**90.1**	**197.8**		**197.8**		**44.50**
THD	$Mm^{-1}\,10\,yr^{-1}$	**−0.6**			**−0.8**			**Negative**	
	$\%\,10\,yr^{-1}$	**−133.1**			**−171.9**				
Europe									
FKL	$ng\,m^{-3}\,10\,yr^{-1}$	**166.1**			−70.1			**Negative**	
	$\%\,10\,yr^{-1}$	**46.2**			−20.6				
HPB	$ng\,m^{-3}\,10\,yr^{-1}$	**−43.8**	−31.6	21.1	**−118.6**	**−124.0**	11.6	**Negative**	
	$\%\,10\,yr^{-1}$	**−16.3**	−11.4	7.7	**−44.0**	**−44.9**	4.2		**−5.87**
JFJ	$Mm^{-1}\,10\,yr^{-1}$	−0.0		0	−0.0		−0.0	No trend	
	$\%\,yr^{-1}$	−0.2		0.0	−1.0		−1.0		5.95
MHD	$\mu g\,m^{-3}\,10\,yr^{-1}$	0.0		0.0	−0.0		−0.0	No trend	
	$\%\,10\,yr^{-1}$	1.8		1.8	−20.4		−20.4		13.34
Arctic and Antarctic									
BRW	$Mm^{-1}\,10\,yr^{-1}$	**−0.02**		**−0.11**	**−0.1**		**−0.1**	**Negative**	
	$\%\,10\,yr^{-1}$	**−13.3**		**−64.7**	**−55.6**		**−76.5**		**−27.90**
NMY	$ng\,m^{-3}\,10\,yr^{-1}$	**−0.01**		**−0.01**	**−0.7**		**−0.7**	No trend	
	$\%\,10\,yr^{-1}$	**−0.7**		**−0.7**	**−58.8**		**−58.8**		−2.42

discrepancies between the MK and GLS/ARB trends, principally for b. For some sites (BRW, NMY, PAL), gaps in the 450 nm or 700 nm σ_{sp} do not allow calculation of b and $å$ values for all wavelengths/wavelength pairs. For other stations (HPB, JFJ, MHD and SPO), clear break points in the b and $å$ series prevented evaluation of the trends in these parameters. This is why trends for b and $å$ are derived for 7 stations only (BND, BRW, MLO, NMY, PAL, SGP and THD).

- No consistent, s.s. trends in b were observed for most of the stations (BND, NMY, PAL, SGP and THD) (Table 6, Fig. 7) when the MK method was used. At BRW and MLO s.s. negative trends in b were found for the 2001–2010 period of approximately −1 and $-3.5\,\%\,yr^{-1}$, respectively, using both MK and GLS/ARB methods. Significant positive trends were found for BND, SGP and THD and negative trends for PAL when the GLS/ARB and LMS methods were used. These negative trends were consistent for both methods, although the two methods were not in agreement about the level of the significance of the trends for every wavelength.

- Similar to the trends found for b, s.s. negative $å$ trends were also found for MLO and BRW regardless of the analysis method used (Table 7, Fig. 7). Similar to the findings for b, no s.s. $å$ trends were found for BND, NMY, PAL, SGP or THD using the MK method, whereas s.s. negative trends were found for PAL and SGP when using GLS/ARB and LMS methods. For NMY and THD, trends with different signs and levels of significance were found for the three analysis methods, but the results based on the MK method should be considered most relevant since the MK method is best able to deal with the known imperfections in the data sets (gaps, negative values, outliers, etc.). There is a clear correlation between the seasonality of σ_{sp} and b and $å$ trends at MLO (Fig. 8): most of the monthly positive σ_{sp} trends also have negative b and $å$ trends suggesting a shift of the aerosol size distribution towards the larger end of the accumulation mode.

Negative b trends signify a relative shift towards larger particles at the lower end of the accumulation mode ($D_p < 0.4\,\mu m$); larger particles being added to the aerosol would have a similar effect on b as smaller particles being removed. A positive b trend would indicate an increased influence on σ_{sp} by smaller particles ($D_p < 0.4\,\mu m$), but not necessarily an increase in the concentration of smaller particles. A negative $å$ trend suggests a shift of the accumulation mode particles towards larger sizes, $å$ being more sensitive to the large end of the accumulation mode ($0.5\,\mu m < D_p < 0.8\,\mu m$) (Collaud Coen et al., 2007). The only two stations (BRW and MLO) with s.s. trends corroborated by at least MK and GLS/ARB tend therefore to measure a decreased influence on σ_{sp} by particles with $D_p < 0.8\,\mu m$ due to greater proportion of large particles relative to smaller particles.

Table 6. Significance and slope of the trends of the backscatter fraction; the labels are similar to Table 3.

Station	Wavelength (nm)	MK (% 10 yr^{-1})			GLS/ARB (% 10 yr^{-1})			LMS	
		All	15 yr	10 yr	All	15 yr	10 yr	Significance, all	Change 2001–2010 (%)
US									
BND	450	−1.4	−1.4	17.3	4.4	4.4	**7.9**	No trend	**2.32**
	550	2.0	2.0	99.3	**7.7**	**7.7**	**10.4**	Positive	1.80
	700	−2.0	−2.0	33.1	**12.8**	**12.8**	**18.3**	**Positive**	**5.46**
MLO	450	**−32.7**		**−32.7**	**−38.7**		**−38.7**	**Negative**	**−16.45**
	550	**−38.0**		**−38.0**	**−44.4**		**−44.4**	**Negative**	**−12.70**
	700	−1.5		−1.5	**−25.1**		**−25.1**	**Negative**	**−6.27**
SGP	450	−4.6		16.6	**6.7**		−0.1	**Positive**	−0.18
	550	17.2		87.6	**7.8**		2.2	**Positive**	0.45
	700	13.9		3.7	**9.2**		**4.2**	**Positive**	1.47
THD	450	−107.9			1.5			No trend	
	550	−73.9			**2.9**			**Positive**	
	700	−11.8			**4.3**			**Positive**	
Europe									
PAL	450	310.8		177.6	**−34.5**		**−34.5**	**Negative**	**−11.72**
	550	30.9		115.2	**−6.3**		**−6.3**	**Negative**	**−4.35**
	700	*							
Arctic and Antarctic									
BRW	450	**−2.3**		**−13.9**	**−6.0**		**−47.4**	No trend	**−7.20**
	550	−1.1		**−8.7**	8.3		0.2	No trend	**−6.48**
	700	*							
NMY	450	*							
	550	37.6		37.6	**−151.7**		**−151.7**	**Negative**	−8.14
	700	**−3.2**		**−3.2**	**12.0**		**12.0**	No trend	−1.33

* Indicates a measurement gap or break point for one wavelength was detected and the trend analysis could not be determined for this wavelength.

4 Discussion

Overall, the derived trends are consistent with the strong decrease in emissions of particulate matter (PM) and SO_2 observed in OECD (Organisation for Economic Co-operation and Development) countries and resulting from air quality regulation and improving technologies in most industrial processes. The decreasing trends are also consistent with trends of aerosol chemistry derived from observations in urban environments in the US and the Europe (EPA, 2011; EEA, 2011) and with derivation of trends for aerosol chemistry for the Europe (Tørseth et al., 2012) and US (Hand et al., 2012). They also generally agree with trends derived from sunphotometer observations (Yoon et al., 2012). There are, however, specific cases where the effect of decreasing emissions is not reflected in the scattering and absorption coefficient trends. In those cases, it is necessary to further explore the station specifics (location, local influences, etc.) to understand the observed optical property trends.

Comparisons with other aerosol properties (e.g. number, mass, chemistry, optical depth), as mentioned above, can provide insight into observed trends, however, there are limitations to this approach as well. Seinfeld and Pandis (1998) present a simple series of graphs (their Fig. 7.6) showing the sensitivity of particle number, surface area (proportionally to scattering) and volume (proportional to mass) to particle size distribution. These figures show that trends in mass will be more sensitive to the large particles ($> 1\,\mu m$) while scattering is more sensitive to the accumulation mode (~ 0.1–$1\,\mu m$). Trends in mass (PM are measured as mass concentration) may therefore not reflect long-term changes in aerosol optical properties. Similarly, the number concentration is dominated by the Aitken and accumulation mode, so a small change in the number concentration of the accumulation mode or coarse mode would not be noticed in N, but could significantly affect the aerosol optical properties. Surveys of aerosol chemical composition suggest that at many locations sulfate makes up only 30–50 % of aerosol mass (e.g. Hand et al., 2012; Zhang et al., 2007) while organics are the other major aerosol constituent by mass. Thus trends in sulfate and scattering are likely to be correlated, but changes in the amounts of other chemical constituents

Table 7. Significance and slope of the trends of the light scattering Ångström exponent; the labels are similar to Table 3.

Station	Wavelength pair (nm)	MK (% 10 yr^{-1})			GLS/ARB (% 10 yr^{-1})			LMS	
		All	15 yr	10 yr	All	15 yr	10 yr	Significance, all	Change 2001–2010 (%)
US									
BND	450–700	13.3	13.3	10.6	0.7	0.7	0.2	No trend	0.54
	450–550	6.8	6.8	−42.8	0.9	0.9	**2.3**	No trend	**1.50**
	550–700	12.2	12.2	9.0	0.6	0.6	−1.2	No trend	−0.47
MLO	450–700	**−30.7**		**−30.7**	**−53.5**		**−53.5**	**Negative**	**−14.69**
	450–550	**−43.1**		**−43.1**	**−69.4**		**−69.4**	**Negative**	**−21.95**
	550–700	**−24.5**		**−24.5**	**−42.6**		**−42.6**	No trend	−8.02
SGP	450–700	−13.4	−13.4	−42.0	**−4.2**	**−4.2**	**−7.7**	**Negative**	**−4.40**
	450–550	−6.2	−6.2	10.7	**−3.1**	**−3.1**	**−4.7**	**Negative**	**−2.55**
	550–700	−16.6	−16.6	−41.6	**−5.0**	**−5.0**	**−8.8**	**Negative**	**−6.02**
THD	450–700	−14.3			9.9			No trend	
	450–550	−36.3			**−13.0**			**Negative**	
	550–700	11.3			**34.4**			**Positive**	
Europe									
PAL	450–700	13.5		8.2	**−11.7**		**−11.9**	**Negative**	**−8.86**
	450–550	*							
	550–700	*							
Arctic and Antarctic									
BRW	450–700	*							
	450–550	**−24.6**		**−10.8**	**−45.1**		**−60.2**	**Negative**	**−31.93**
	550–700	*							
NMY	450–550	*							
	550–700	*							
	550–700	27.6		28.5	**−14.3**		**−14.3**	No trend	−0.33

* Indicates a measurement gap or break point for one wavelength was detected and the trend analysis could not be determined for this wavelength pair.

can also affect optical property trends. Likewise, spatial inhomogeneities (both horizontal and vertical) may result in discrepancies between in situ aerosol optical properties and other aerosol properties. For example, trends in aerosol optical depth may be strongly correlated with surface extinction measurements at some sites (e.g. Hand et al., 2004) because the column aerosol is often dominated by aerosol loading near the surface, however, variability of the aerosol vertical profile (i.e. layers) can confound the relationship between surface and column extinction (e.g. Bergin et al., 2000).

4.1 Connection between observed trends in optical properties and emission reductions in Europe andthe continental US

It seems very likely that emission reductions are the primary driver for the observed trends, in particular over the continental US, where negative trends were found for the three GAW stations measuring at least 2 aerosol parameters (BND, SGP and THD) both over the entire station record and for the last ten years. Decreases in scattering were also observed for almost all IMPROVE stations with the exception of three desert influenced stations in Arizona (HGC, IBB, SCN) and the high altitude site of MZW. The non-significant or positive trends found in Arizona, and some high altitude sites may be related to different regional aerosol sources and/or to long-range transport and this is described in more detail in Sect. 4.2.

In the US, estimates of emission reductions since 2000 are of the order of 50 % for $PM_{2.5}$ and 55 % for SO_2 (EPA, 2011). Reductions are slightly less for other particle precursors such as VOCs and NO_x (−35 % and −41 % since 2000, respectively). These decreasing trends are consistent with Murphy et al. (2011), who found negative trends in $PM_{2.5}$ for almost all IMPROVE stations. These decreases in the US from 2000-2009 are stronger than the decreases in Europe over the same time period (Tørseth et al., 2012; Hand et al., 2012b). The anthropogenic SO_2 emission decrease (see Fig. 5 in the companion paper Asmi et al., 2013) is much more pronounced in North America (−5 to −10 % yr^{-1}) below 45° N for the 2000–2008 period than it was in Europe over the same time period (0 to −3 % yr^{-1}).

In Europe, s.s. decreasing trends for σ_{sp} are observed only for FKL and can be related to regional conditions. No s.s. trends in scattering were found for the other four European sites. There have been, however, considerable changes in European sulfur and PM emissions over the period 1980–2010. Decreases in $PM_{2.5}$ emissions since 2000 are estimated to be of the order of 12 % (1 % yr^{-1}) while the decrease in SO_2

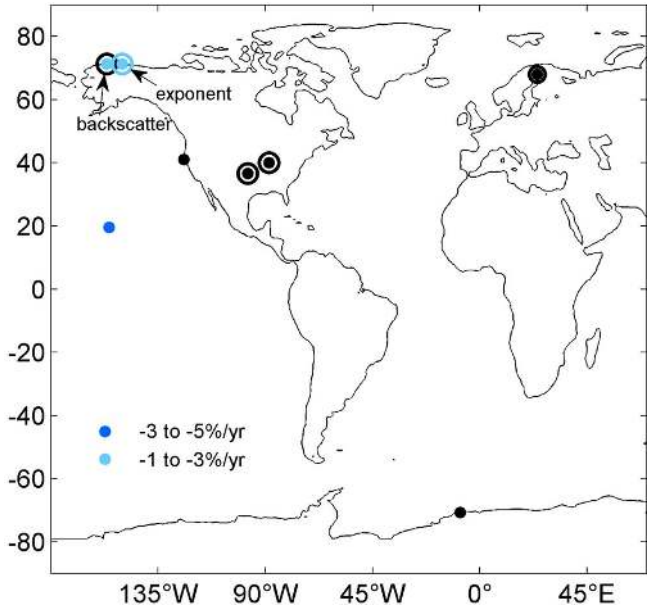

Fig. 7. Mann-Kendall trend results for the backscatter fraction and the scattering Ångström exponent calculated from the daily medians of the scattering coefficients. All stations apart from BRW had the same trends for both parameters. The symbols have the same meaning as in Fig. 4.

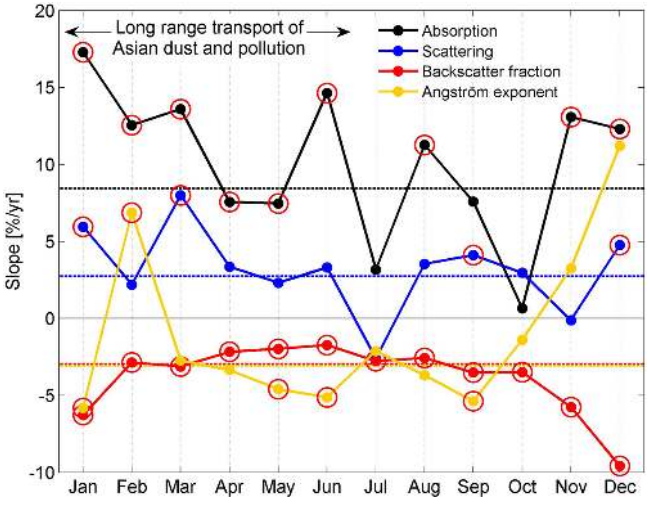

Fig. 8. Seasonal Mann-Kendall trend analysis for the MLO scattering and absorption coefficient as well as the backscatter fraction and the scattering Ångström exponent. The symbols have the same meaning as in Fig. 5.

is estimated to be similar to continental US (50 % decrease since 2000) (EEA, 2011). Tørseth et al. (2012) showed that the SO_x emissions decreased by 11 % over the last decade, whereas in the two previous decades (1990–1999 and 1980–1989) SO_x emissions decreases were much larger, 40 % and 21 %, respectively. Figure 5 of the companion paper (Asmi et al., 2013) also shows a mean decrease of about 2 % yr^{-1} in anthropogenic SO_2 and a slightly weaker decrease in PM, in accordance with the observations reported to EMEP (Tørseth et al., 2012). All of the significant $PM_{2.5}$ and PM_{10} trends observed in Europe were negative, with slopes between −2 and −4 % yr^{-1}, but no s.s. trends were observed for about half of the data sets (6 out of 13 for $PM_{2.5}$ and 13 out of 23 for PM_{10}). Thus, about half of the EMEP stations did not have significant trends over the last decade, covering most of the time period for the optical property trends described here.

HPB is the only central European site in this study located with a strong influence from continental boundary layer air (JFJ is frequently above the PBL, MHD and FKL are marine sites and PAL is in northern Europe). Conveniently, Tørseth et al. (2012) reported observed trends of PM and sulfate at HPB, which can be compared with the trends in σ_{ap} and σ_{sp} reported here. A decreasing trend in PM is not observed at HPB over the past 10 yr and is strongly influenced by the very high values of 2003 (an extremely hot and dry summer over Europe). This is consistent with the lack of trends observed in scattering and absorption for the 10 yr period. As mentioned above there was a larger emissions decrease in western Europe in the 1990–2000 period relative to the decrease observed for the 2000–2009 period. This corresponds with our observation that there is a s.s. decreasing trend in the 16 yr absorption coefficient record at HPB, which is not detectable if just the last 10 yr are evaluated. The HPB scattering record begins in 2002 so we cannot compare it with the longer absorption and PM_{10} trends.

The effect of decreasing emissions is not observed at the high altitude site JFJ in either the scattering or absorption signal, regardless of the statistical method used. The JFJ station is often in the free troposphere, but is influenced by the PBL during the summer as well as in cases of lifting or subsidence synoptic weather types. A previous study (Collaud Coen et al., 2007) has shown that over the period 1995–2005 no s.s. trends were observed for aerosol optical properties during the summer months, whereas increasing trends were observed for the fall months, which are more representative of FT air masses. In the present analysis, August is the only month with a s.s. negative trend for both HPB and JFJ stations and for both σ_{sp} and σ_{ap}; August is also the month with the warmest temperatures and maximal PBL influence. The August trend provides the only evidence found at the JFJ for the particulate and gaseous emission decreases measured over Europe.

In summary, at most US continental sites, decreasing trends observed for aerosol optical properties are generally consistent with SO_2 and PM reductions. For continental European sites, the relation between aerosol optical properties and emissions reductions is less clear. The strong decreasing signal observed in Tørseth et al. (2012) for SO_2 and, with a lower spatial homogeneity and statistical significance, for $PM_{2.5}$ was not observed for aerosol optical properties

in Europe. As mentioned above spatial inhomogenieties can limit the direct comparison of aerosol optical properties trends with other aerosol property trends, and here the European discrepancy might also be due to under-representation of continental Europe PBL sites in our study. Furthermore, the difference in the timing of SO_2 and PM trends for the two continents (e.g. in contrast to the US, the Europe emissions reductions were greater for the 1980–2000 period than during the last decade) is another likely explanation for the decreasing trends in aerosol number concentration and optical parameters found for most American sites compared to the lack of trends observed in Europe. The European optical property time series may not go back far enough to reflect the time period largest emission reductions.

Finally, optical properties at the Arctic and Antarctic stations do not appear to be influenced by increases in anthropogenic pollution. Decreasing trends in absorption coefficient were found at both BRW and NMY stations and σ_{sp} trends were non-significant at all three sites. In the Antarctic, the optical property trends were not consistent with the increasing trends found for N (Asmi et al., 2013) for the 2000–2010 time period. The inconsistency in the N and scattering trends in Antarctica is likely due to the two parameters being sensitive to different parts of the size distribution. At NMY, Weller et al. (2011) found no significant trends in any aerosol chemical constituents except for nitrate, which decreased throughout the 1993–2000 period and subsequently levelled out. Aerosol property trends in the polar regions should be revisited in a few years as changes in those regions may begin to be reflected in the aerosol parameters. For example, Sharma et al. (2012) found increasing methanesulfonic acid (MSA) in the Arctic which they suggested could be due to less sea ice/more open water.

4.2 Specific case of stations with positive trends for scattering and/or absorption

There were several sites with increasing trends in scattering and/or absorption. In the US these include some but not all high altitude sites and some but not all desert sites. In Europe positive trends were seen for at least one variable at each marine site. Here we look more closely at the characteristics of each site to try to explain these observations and also discuss what we would need to know to more closely diagnose the positive trends.

The high altitude MLO site in the middle of the Pacific Ocean has the only data set suggesting an increase of both the scattering and absorption coefficients over the last ten years. This increase is associated with an increase in particle size indicated by a decrease in both $å$ and b. In contrast, a s.s. decreasing trend is found for N at MLO. Yoon et al. (2012) report an increase of 1–2 % yr^{-1} in column AOD measured by ground based observations (AERONET) at MLO, although they note that the MLO trends may be insignificant because the measured AOD values are close to the observation uncertainty. Additionally, the Yoon et al. (2012) AOD trends are not directly comparable with the in situ trends as sun photometers measure during the daytime, while the in-situ data (screened to remove upslope air) represent primarily a nighttime data set. The seasonality of the trends at MLO is also noteworthy (Fig. 8) particularly for the absorption coefficient. Significant positive trends were found during the January–June period, consistent with the monthly frequency of long-range transport of Asian dust and pollution (Bodhaine, 1983; Perry et al., 1999; Eck et al., 2005; VanCuren and Cahill, 2002). Correlations with the positive trend of anthropogenic SO_2 and PM_{10} emission over the ocean as well as of PBL height (Asmi et al., 2013, Fig. 5) are also obvious and may be relevant to the observed increase in scattering and absorption coefficients. An increase in absorption coefficient is often connected with an increased influence of anthropogenic pollution and/or biomass burning. Since data influenced by local pollution sources (i.e. samples measured during upslope conditions) are removed from the MLO data set during the QC process, the most probable cause of the positive trends in absorption and scattering is the increased emission of pollutants in Asia being partially lifted and transported by high altitude winds to reach MLO. To better understand the observed trends (decreasing trend in N, along with increasing trends in σ_{sp}, σ_{ap} and increasing particle size) information about the source(s) of the observed air masses (e.g. regional lifting versus long-range transport), the chemical fingerprint of the airmass (e.g. biomass burning tracers) and perhaps changes in biomass burning/pollutions emissions in Asia would be helpful.

While the increasing trends at MLO are most likely caused by changes in sources and/or transport, the s.s. increasing scattering trends at MZW and IBB are contradicted by other measurements made at these sites (e.g. chemistry, mass and extinction calculated from measured aerosol chemistry), thus, we cannot hypothesize about reasons for the observed increasing trends. The MZW scattering measurements ended in 2009, however, a new series of optical measurements began in 2011 at Storm Peak Laboratory (SPL) which is in the same region at MZW. These new optical measurements in conjunction with longer term aerosol physical property measurements at (SPL) may help to resolve the MZW puzzle in 5–10 yr.

Completely different trends in aerosol optical properties were observed for the two marine stations in Europe (FKL and MHD) compared to those found for the continental sites. No trend in absorption coefficient was detected at MHD, which can be attributed to minimal anthropogenic influence at the site. The increase in σ_{sp} at MHD is surprising and cannot be explained by a corresponding increase in RH (the relative humidity is controlled and, moreover, the RH trend is negative and not significant). The positive σ_{sp} trend is opposite to the negative trend in N observed for MHD (Asmi et al., 2013), suggesting changes sources affecting different parts of the aerosol size distribution. Again, comparison with

Tørseth et al. (2012) for this region shows that (a) the decreasing PM signal is not s.s. for MHD and (b) that some UK sites exhibit a positive PM trend. We have, however, no explanation in terms of aerosol emissions changes, for the increasing scattering trend observed at MHD and further investigation is necessary. Some possibilities include a trend towards increasing wind speed, which would increase scattering from sea salt, and/or changes in the relative amount of continental vs. marine air masses reaching MHD. At FKL, the negative σ_{sp} trend is mostly due to biomass burning in the area early in the data set, leading to especially high scattering values in the 2001–2003 period. The absorption measurements began in 2003 and were therefore not influenced by the smoke events. If the FKL σ_{sp} data set is restricted to 2003–2010, the scattering trend also becomes positive but the trend is not significant.

4.3 Influence of regional aerosol sources and transport modalities

Aerosol property trends in the southwestern US appear to be more variable than in other parts of the country. In general the trends are less negative for the western US and in some cases even positive (IBB and MZW, this study; Murphy et al., 2011 (for $PM_{2.5}$); Xia et al., 2011 (for AOD); Augustine et al., 2008 (for AOD); Hand et al., 2012b (for $PM_{2.5}$, PM_{10}, coarse mass and soil)). While emissions reductions may contribute to downward trends in the region for some aerosol species (e.g. sulfate, Hand et al., 2011, 2012b), increases in other types of emissions may counteract the negative trends. For example, hotter, drier conditions in the southwest US as well as changes in land use may have resulted in increased forest fires and changes in dust emissions (e.g. Westerling et al., 2006; Reheis and Urban, 2011). Similarly, Sorooshian et al. (2011) focused specifically on southern Arizona and found decreasing trends in most aerosol chemical constituents except dust for the region. There is also a well-defined seasonality in the type of aerosols influencing this region (Sorooshian et al., 2011; Hand et al., 2012). From March to July mineral dust dominates, while in May–August large wildfire activity and organic aerosols also contribute. Figure 9 shows the seasonality of the trends for the 5 Arizona stations potentially influenced by desert dust (IBB, PAZ, SIA, SCN, and HGC) and also indicates the timing of fire and dust emissions. The negative trends found for PAZ and SIA are largest when the dust influence is the lowest (i.e. winter). SCN has no overall trend due to non-significant negative trends in winter and positive trends observed during dust influenced months. HGC has also an overall non-significant trend due to alternating positive trends (February–July) and negative trends (September to November). We can therefore clearly observe negative trends at these sites during the months with low dust influence consistent with other continental US sites, whereas non-significant or positive trends occur during the months with more dust influence consistent

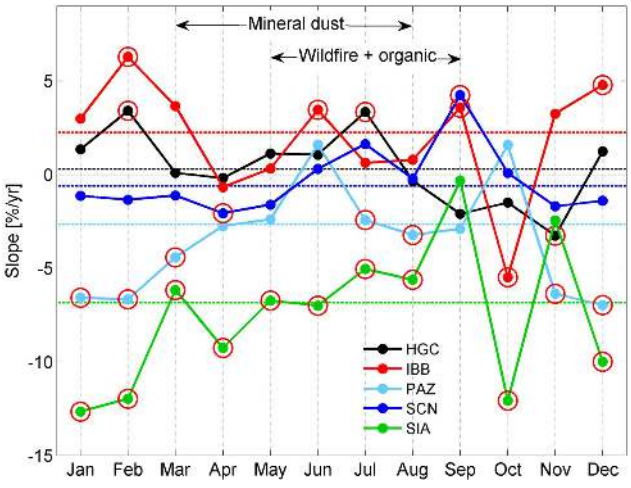

Fig. 9. Seasonal Mann-Kendall trend analysis for the scattering coefficients of southwestern US (Arizona) stations. The symbols have the same meaning as in Fig. 5.

with the results of Sorooshian et al. (2011). Only the positive trends at IBB that are maximal in November–December and February–March cannot be clearly related to the known aerosol sources seasonality. The southwestern US aerosol optical property trends illustrate the seasonality of aerosol sources and the variability of the local influence of different aerosol species on aerosol optical properties.

Finally, no direct link between either scattering or absorption trends and the geographical classification of the station (e.g. marine versus continental, or low versus high altitude) was found. For example, the five Arizona stations are situated at different elevations (372 to 2267 m a.s.l.), but no relationship between altitude and slope of trend was found. No coherent trends were found for the six US desert sites. In Europe, the trends observed for the two marine stations (MHD and FKL) are mostly influenced by different aerosol sources, whereas trends for the two US marine stations (ACA and THD) are consistent with most other US continental sites. In addition, no consistent trends in scattering were observed at the highest sites: no s.s. trends were observed for JFJ at 3580 m, HGC at 2267 m, SCN at 2046 m and SPO at 2410 m but s.s. positive trends were found for both MLO at 3400 m a.s.l. and MZW at 3243 m a.s.l. No negative trends were found for these high altitude stations, which sample (at least part of the time) in the FT. We therefore cannot conclude that high altitude stations are less sensitive to changes than stations sampling from the PBL, but that they are representative of other aerosol sources, transport modalities or atmospheric processes.

Table 8. Overview of scattering and absorption decadal (2001–2010) trends per continent/region of the world.

Region (nb of stations/nb of stations with s.s. trend)	Mean trend for all stations (% yr^{-1}) (std)	Mean trend for stations with s.s. trend (% yr^{-1}) (std)
Scattering coefficient		
US (14/10)	−2.0 (2.5)	−2.9 (2.4)
Europe (4/1)	+0.6 (1.9)	+2.7
Mauna Loa (1/1)	+2.7	+2.7
Arctic (1/0)	+2.4	
Antarctic (1/0)	+2.5	
Absorption coefficient		
US (1/1)	−2.0	−2
Europe (3/0)	−0.3 (0.4)	
Mauna Loa (1/1)	+9.0	+9.0
Arctic (1/1)	−6.5	−6.5
Antarctic (1/1)	−0.07	−0.07

5 Conclusions

To our knowledge, this is the first time that trends for these aerosol climate variables are derived from stations with large spatial representation. The emerging picture is, first of all, that the number of stations providing data sets of sufficient duration for performing s.s. analyses is, currently, limited (24 stations worldwide as opposed to the larger number of stations contributing to GAW and WDCA). Despite recent efforts to increase the number of observing stations and the data quality, this remains problematic for providing a global picture. The highly variable signals of absorption and scattering coefficients (as well as for N as shown in Asmi et al., 2013) require multi-year records longer than 8 yr to derive s.s. trends. Clearly, a similar analysis performed in 5–10 yr will include a much larger number of stations, particularly in Europe, but also a few sites in Asia and Africa (assuming that all current observing sites remain active).

Results from this study provide evidence that aerosol optical properties have significantly changed at many locations over the last 10 and 15 yr. It is also clearly evident that the derived trends are not spatially homogenous and result from complex processes that possibly include changes in emission source intensities, transport efficiency (including removal) and transformation of aerosol particles. In the context of the present paper, changes in transport patterns and transformation (e.g. condensation) were not investigated. The expectation from this long-term trend analysis is that decreasing emissions over the last decades of primary particles and particulate precursors such as SO_2 would have led to significant decreases of both aerosol absorption and scattering coefficients. This tendency is clearly observed over the continental US where scattering is decreasing at a mean rate of $-2\,\%\,yr^{-1}$ over the last 10 yr (Table 8), slightly lower than the estimated rates of decrease for primary particle and SO_2 emissions. The absorption signals also show a general decrease in the US but the analysis is made on a limited number of data sets (one station with $-2.0\,\%\,yr^{-1}$ over the last 10 yr). Surprisingly, trends derived from Europe sites did not show a similar decrease, despite efficient emission abatement policies. In the Europe, significant trends were not observed for aerosol optical properties at most sites, with a few exceptions (see Table 8). This may be due to differences in the time period for major European reductions relative to the time period covered by the aerosol optical property measurements, but it may also be a result of the limited number of data sets (five stations available for scattering coefficient and only four for absorption coefficient, (four and three, respectively, for the 2001–2010 period) as well as from the characteristics of the sites (e.g. high altitude or marine).

The analysis also suggests findings for some locations that may need additional investigation, e.g. sites where the scattering and/or absorption signals indicate increasing trends of a few $\%\,yr^{-1}$. This is the case, for example, for the MLO free troposphere station in the Pacific, possibly under the influence of stronger emission intensity from Eastern Asia, and, more surprisingly, for the MHD marine station in Europe and the MZW high altitude station in continental US. More focused studies documenting the stations' regional environments are required to explain the specific results. It is clear however that despite the general decrease in anthropogenic emissions in OECD countries, some stations in continental Europe and US or in the high latitude regions show trends that are not consistent with emissions decrease. The evolution of the aerosol properties in the atmosphere results from highly non-linear mechanisms as shown in recent studies (Kulmala et al., 2011). The analysis of the seasonal trends at some stations provides an insight to this complexity. Some of the results obtained in this study are consistent with the hypothesis that climate-related changes may be acting on natural source emission (increase in biomass burning emissions in Continental US) or on local transport (thermal winds at JFJ) and may already have affected the overall trends. Additional information that will help for identifying causes for increasing trends may be derived from the analysis of backscatter fraction and the scattering Ångström exponents. At present, however, even though trends were derived for a few stations, spatial representativity of results is too scarce to provide global conclusions. Clearly, additional studies are needed to better understand causes for the observed trends.

Repeating this analysis in the future with more stations and longer-duration records is clearly warranted. It is, however, fundamental to emphasize the need for quality control on data sets to perform such trend analyses. Quality control procedures can only be implemented with skilled personnel at the stations and within a coordinated international effort for ensuring coherence of operating procedures and data reduction treatments; use of long-term data sets will remain problematic without such efforts. Finally, we would like to emphasize again the need for additional information outside the regions covered by this study to derive a global picture of

the evolution of the atmospheric aerosol properties and their role in climate change.

Supplementary material related to this article is available online at: http://www.atmos-chem-phys.net/13/869/2013/acp-13-869-2013-supplement.pdf.

Acknowledgements. The authors would like to thank the numerous, but unfortunately unnamed, technical and scientific staff members of the stations included in these analyses, whose dedication to quality for decades have made this paper possible. We also thank the International Foundation High Altitude Research Stations Jungfraujoch and Gornergrat (HFSJG), which made it possible to carry out the experiments at the High Altitude Research Station at the Jungfraujoch and the support by MeteoSwiss within the Swiss program of the Global Atmosphere Watch (GAW) of the WMO. European sites and measurements were also supported by the Co-operative Programme for Monitoring and Evaluation of the Long-range Transmission of Air pollutants in Europe (EMEP) under UNECE. The research leading to these results has received funding from the European Union Seventh Framework Programme (FP7/2007–2013) under the ACTRIS project with grant agreement #262254 as well as from the Europe FP6 project *European Supersites for Atmospheric Aerosol Research* (EUSAAR) and the Europe FP5 project *Construction*, use and delivery of an European aerosol database (CREATE).

Edited by: M. C. Facchini

References

Anderson, T. L. and Ogren, J. A.: Determining aerosol radiative properties using the TSI 3563 integrating nephelometer, Aerosol Sci. Tech., 29, 57–69, 1998.

Anderson, T. L., Masonis, S. J., Covert, D. S., Ahlquist, N. C., Howell, S. G., Clarke, A. D., and McNaughton, C. S.: Variability of aerosol optical properties derived from in situ aircraft measurements during ACE-Asia, J. Geophys. Res., 108, 8647, doi:10.1029/2002JD003247, 2003.

Andrews, E., Ogren, J. A., Bonasoni, P., Marinoni, A., Cuevas, E., Rodriguez, S., Sun, J. Y., Jaffe, D. A., Fischer, E. V., Baltensperger, U., Weingartner, E., Collaud Coen, M., Sharma, S., Macdonald, A. M., Leaitch, W. R., Lin, N.-H., Laj, P., Arsov, T., Kalapov, I., Jefferson, A., and Sheridan, P. J.: Climatology of aerosol radiative properties in the free troposphere, Atmos. Res., 102, 365–393, 2011.

Asmi, A., Wiedensohler, A., Laj, P., Fjaeraa, A.-M., Sellegri, K., Birmili, W., Weingartner, E., Baltensperger, U., Zdimal, V., Zikova, N., Putaud, J.-P., Marinoni, A., Tunved, P., Hansson, H.-C., Fiebig, M., Kivekäs, N., Lihavainen, H., Asmi, E., Ulevicius, V., Aalto, P. P., Swietlicki, E., Kristensson, A., Mihalopoulos, N., Kalivitis, N., Kalapov, I., Kiss, G., de Leeuw, G., Henzing, B., Harrison, R. M., Beddows, D., O'Dowd, C., Jennings, S. G., Flentje, H., Weinhold, K., Meinhardt, F., Ries, L., and Kulmala, M.: Number size distributions and seasonality of submicron particles in Europe 2008–2009, Atmos. Chem. Phys., 11, 5505–5538, doi:10.5194/acp-11-5505-2011, 2011.

Asmi, A., Collaud Coen, M., Ogren, J. A., Andrews, E., Sheridan, P., Jefferson, A., Weingartner, E., Baltensperger, U., Bukowiecki, N., Lihavainen, H., Kivekäs, N., Asmi, E., Aalto, P. P., Kulmala, M., Wiedensohler, A., Birmili, W., Hamed, A., O'Dowd, C., Jennings, S. G., Weller, R., Flentje, H., Mari Fjaeraa, A., Fiebig, M., Lund Myhre, C., Hallar, A. G., Swietlicki, E., Kristensson, A., and Laj, P.: Aerosol decadal trends – Part 2: In-situ aerosol particle number concentrations at GAW and ACTRIS stations, Atmos. Chem. Phys., 13, 895–916, doi:10.5194/acp-13-895-2013, 2013.

Augustine, J. A., Hodges, G. B., Dutton, E. G. Michalsky, J. J., and Cornwall, C. R.: An aerosol optical depth climatology for NOAA's national surface radiation budget network (SURFRAD), J. Geophys. Res., 113, D11204, doi:10.1029/2007JD009504, 2008.

Barmpadimos, I., Hueglin, C., Keller, J., Henne, S., and Prévôt, A. S. H.: Influence of meteorology on PM_{10} trends and variability in Switzerland from 1991 to 2008, Atmos. Chem. Phys., 11, 1813–1835, doi:10.5194/acp-11-1813-2011, 2011.

Bayazit, M. and Önöz, B.: To prewhiten or not to prewhiten in trend analysis?, Hydro. Sci. J., 5, 611–624, doi:10.1623/hysj.52.4.611, 2007.

Bergin, M. H., Schwartz, S. E., Halthore, R. N., Ogren, J. A., and Hlavka, D. L.: Comparison of aerosol optical depth inferred from surface measurements with that determined by Sun photometry for cloud-free conditions at a continental US site, J. Geophys. Res., 105, 6807–6816, 2000.

Bodhaine, B.: Aerosol Measurements at Four Background Sites, J. Geophys. Res., 88, 10753–10768, 1983.

Bodhaine, B. A. and Dutton, E. G.: Long-term decreases in arctic haze at Barrow, Alaska, Geophys. Res. Lett., 20, 947–950, 1993.

Bond, T. C., Anderson, T. L., and Campbell, D.: Calibration and intercomperison of filter-based measurements of visible light absorption by aerosols, Aerosol Sci. Tech., 30, 582–600, 1999.

Charlson, R. J., Schwartz, S. E., Hales, J. M., Cess, R. D., Coakley, Jr., J. A., Hansen, J. E., and Hoffman, D. J.: Climate forcing by anthropogenic aerosols, Science, 255, 423–430, doi:10.1126/science.255.5043.423, 1992.

Collaud Coen, M., Weingartner, E., Nyeki, S., Cozic, J., Henning, S., Verheggen, B., Gehrig, R., and Baltensperger, U.,: Long-term trend analysis of aerosol variables at the high-alpine site Jungfraujoch, J. Geophys. Res., 112, D13213, doi:10.1029/2006JD007995, 2007.

Collaud Coen, M., Weingartner, E., Apituley, A., Ceburnis, D., Fierz-Schmidhauser, R., Flentje, H., Henzing, J. S., Jennings, S. G., Moerman, M., Petzold, A., Schmid, O., and Baltensperger, U.: Minimizing light absorption measurement artifacts of the Aethalometer: evaluation of five correction algorithms, Atmos. Meas. Tech., 3, 457–474, doi:10.5194/amt-3-457-2010, 2010.

Conrad, V. and Pollak, L. W.: Methods in Climatology, Harvard University Press, Boston, 1950.

Day, D. E. and Malm, W. C.: Aerosol light scattering measurements as a function of relative humidity: a comparison between measurements made at three different sites, Atmos. Environ., 35, 5169–5176, 2001.

Delene, D. J. and Ogren, J. A.: Variability of aerosol optical properties at four north American surface monitoring sites, J. Atmos. Sci., 59, 1135–1150, 2002.

EEA: Air quality in Europe – 2011 report, Technical report No 9/2011, ISSN EEA Technical report series, Copenhagen, Denmark, 1725–2237, doi:10.2800/83213, 2011.

Eck, T. F., Holben, B. N., Dubovik, O., Smirnov, A., Goloub, P., Chen, H. B., Chatenet, B., Gomes, L., Zhang, X.-Y., Tsay, S.-C., Ji, Q., Giles, D., and Slutsker, I.: Columnar aerosol optical properties at AERONET sites in central eastern Asia and aerosol transport to the tropical mid-Pacific, J. Geophys. Res., 110, D06202, doi:10.1029/2004JD005274, 2005.

EMEP: EMEP Status report 4/2010, Transboundary Particulate Matter in Europe, 2010.

EPA: Emissions of primary particulate matter and secondary particulate matter precursors, Assessment published December 2011, available at: http://www.epa.gov/ttn/chief/trends/, CSI 003, 2011.

Fierz-Schmidhauser, R., Zieger, P., Gysel, M., Kammermann, L., DeCarlo, P. F., Baltensperger, U., and Weingartner, E.: Measured and predicted aerosol light scattering enhancement factors at the high alpine site Jungfraujoch, Atmos. Chem. Phys., 10, 2319–2333, doi:10.5194/acp-10-2319-2010, 2010.

Gilbert, R. O.: Statistical Methods for Environmental Pollution Monitoring, Van Nostrand Reinhold Company, New York, 1987.

Gras, J. L.: Baseline atmospheric condensation nuclei at Cape Grim 1977–1987, J. Atmos. Chem., 11, 89–106, 1990.

Hand, J. L. and Malm, W. C.: Review of aerosol mass scattering efficiencies from ground-based measurements since 1990, J. Geophys. Res., 112, D16203, doi:10.1029/2007JD008484, 2007.

Hand, J. L., Kreidenweis, S. M., Slusser, J., and Scott, G.: Comparisons of aerosol optical properties derived from Sun photometry to estimates inferred from surface measurements in Big Bend National Park, Texas, Atmos. Environ., 38, 6813–6821, 2004.

Hand, J. L., Copeland, S. A., Day, D. E., Dillner, A. M., Indresand, H., Malm, W. C., McDade, C. E., Moore, C. T., Pitchford, M. L., Schichtel, B. A., and Watson, J. G., : IMPROVE, Spatial and Seasonal Patterns and Temporal Variability of Haze and its Constituents in the United States, available at http://vista.cira.colostate.edu/improve/Publications/Reports/2011/2011.htm, 2011.

Hand, J. L., Schichtel, B. A., Malm, W. C., and Pitchford, M. L.: Particulate sulfate ion concentration and SO_2 emission trends in the United States from the early 1990's through 2010, Atmos. Chem. Phys., 12, 10353–10365, doi:10.5194/acp-12-10353-2012, 2012a.

Hand, J. L., Schichtel, B. A., Pitchford, M., Malm, W. C., and Frank, N. H.: Seasonal composition of remote and urban fine particulate matter in the United States, J. Geophys. Res., 117, D05209, doi:10.1029/2011JD017122, 2012b.

Henne, S., Brunner, D., Folini, D., Solberg, S., Klausen, J., and Buchmann, B.: Assessment of parameters describing representativeness of air quality in-situ measurement sites, Atmos. Chem. Phys., 10, 3561–3581, doi:10.5194/acp-10-3561-2010, 2010.

Hirdman, D., Burkhart, J. F., Sodemann, H., Eckhardt, S., Jefferson, A., Quinn, P. K., Sharma, S., Ström, J., and Stohl, A.: Long-term trends of black carbon and sulphate aerosol in the Arctic: changes in atmospheric transport and source region emissions, Atmos. Chem. Phys., 10, 9351–9368, doi:10.5194/acp-10-9351-2010, 2010.

Hirsch, R. M., Slack, J. R., and Smith, R. A. : Techniques of trend analysis for monthly water quality data, Water Resour. Res., 18, 107–121, 1982.

IMPROVE: Revised IMPROVE algorithm for estimating light extinction from particle speciation data, available at: http://vista.cira.colostate.edu/improve/Publications/GrayLit/gray_literature.htm, 2006.

Intergovernmental Panel on Climate Change (IPCC): Climate Change 2007: The Physical Science Basis, Contribution of Working Group I to the Fourth Assessment Report of the Intergovernmental Panel on Climate Change, edited by: Solomon, S., Qin, D., Manning, M., Chen, Z., Marquis, M., Averyt, K. B., Tignor, M., and Miller, H. L., Cambridge University Press, Cambridge, United Kingdom and New York, NY, USA, 2007.

Joranger, E. and Ottar, B.: Air pollution studies in the Norwegian Arctic Geophys. Res. Lett., 11, 365–368, doi:10.1029/GL011i005p00365, 1984.

Junker, C., Jennings, S. G., and Cachier, H.: Aerosol light absorption in the North Atlantic: trends and seasonal characteristics during the period 1989 to 2003, Atmos. Chem. Phys., 6, 1913–1925, doi:10.5194/acp-6-1913-2006, 2006.

Kulmala, M., Asmi, A., Lappalainen, H. K., Baltensperger, U., Brenguier, J.-L., Facchini, M. C., Hansson, H.-C., Hov, Ø., O'Dowd, C. D., Pöschl, U., Wiedensohler, A., Boers, R., Boucher, O., de Leeuw, G., Denier van der Gon, H. A. C., Feichter, J., Krejci, R., Laj, P., Lihavainen, H., Lohmann, U., McFiggans, G., Mentel, T., Pilinis, C., Riipinen, I., Schulz, M., Stohl, A., Swietlicki, E., Vignati, E., Alves, C., Amann, M., Ammann, M., Arabas, S., Artaxo, P., Baars, H., Beddows, D. C. S., Bergström, R., Beukes, J. P., Bilde, M., Burkhart, J. F., Canonaco, F., Clegg, S. L., Coe, H., Crumeyrolle, S., D'Anna, B., Decesari, S., Gilardoni, S., Fischer, M., Fjaeraa, A. M., Fountoukis, C., George, C., Gomes, L., Halloran, P., Hamburger, T., Harrison, R. M., Herrmann, H., Hoffmann, T., Hoose, C., Hu, M., Hyvärinen, A., Hõrrak, U., Iinuma, Y., Iversen, T., Josipovic, M., Kanakidou, M., Kiendler-Scharr, A., Kirkevåg, A., Kiss, G., Klimont, Z., Kolmonen, P., Komppula, M., Kristjánsson, J.-E., Laakso, L., Laaksonen, A., Labonnote, L., Lanz, V. A., Lehtinen, K. E. J., Rizzo, L. V., Makkonen, R., Manninen, H. E., McMeeking, G., Merikanto, J., Minikin, A., Mirme, S., Morgan, W. T., Nemitz, E., O'Donnell, D., Panwar, T. S., Pawlowska, H., Petzold, A., Pienaar, J. J., Pio, C., Plass-Duelmer, C., Prévôt, A. S. H., Pryor, S., Reddington, C. L., Roberts, G., Rosenfeld, D., Schwarz, J., Seland, Ø., Sellegri, K., Shen, X. J., Shiraiwa, M., Siebert, H., Sierau, B., Simpson, D., Sun, J. Y., Topping, D., Tunved, P., Vaattovaara, P., Vakkari, V., Veefkind, J. P., Visschedijk, A., Vuollekoski, H., Vuolo, R., Wehner, B., Wildt, J., Woodward, S., Worsnop, D. R., van Zadelhoff, G.-J., Zardini, A. A., Zhang, K., van Zyl, P. G., Kerminen, V.-M., S Carslaw, K., and Pandis, S. N.: General overview: European Integrated project on Aerosol Cloud Climate and Air Quality interactions (EUCAARI) – integrating aerosol research from nano to global scales, Atmos. Chem. Phys., 11, 13061–13143, doi:10.5194/acp-11-13061-2011, 2011.

Laj, P., Klausen, J., Bilde, M., Plaß-Duelmer, C., Pappalardo, G., Clerbaux, C., Baltensperger, U., Hjorth, J., Simpson, D., Reimann, S., Coheur, P.-F. , Richter, A., De Mazière, M., Rudich, Y., Mciggans, G., Torseth, K., Wiedensohler, A., Morin, S., Schulz, M., Allan, J. D., Attié, J.-L., Barnes, I., Birmili, W., Cammas, J. P., Dommen, J., Dorn, H.-P., Fowler, D., Fuzzi, S., Glasius, M., Granier, C., Hermann, M., Isaksen, I. S. A., Kinne, S.,

Koren, I., Madonna, F., Maione, M., Massling, A., Moehler, O., Mona, L., Monks, S., Müller, D., Müller, T., Orphal, J., Peuch, V.-H. , Stratmann, F., Tanré, D. , Tyndall, G., Riziq, A. A., Van Roozendael, M., Villani, P., Wehner, B., Wex, H., and Zardini, A. A.: Measuring atmospheric composition change, Atmos. Environ., 43, 5351–5414 doi:10.1016/j.atmosenv.2009.08.020, 2009.

Leibensperger, E. M., Mickley, L. J., Jacob, D. J., Chen, W.-T., Seinfeld, J. H., Nenes, A., Adams, P. J., Streets, D. G., Kumar, N., and Rind, D.: Climatic effects of 1950–2050 changes in US anthropogenic aerosols – Part 1: Aerosol trends and radiative forcing, Atmos. Chem. Phys., 12, 3333–3348, doi:10.5194/acp-12-3333-2012, 2012.

Mahowald, N. M., Ballantine, J. A., Feddema, J., and Ramankutty, N.: Global trends in visibility: implications for dust sources, Atmos. Chem. Phys., 7, 3309–3339, doi:10.5194/acp-7-3309-2007, 2007.

Malm, W. C., Sisler, J. F., Huffman, D., Eldred, R. A., and Cahill, T. A.: Spatial and seasonal trends in particle concentration and optical extinction in the United States, J. Geophys. Res., 99, 1347–1370, 1994.

Malm, W. C., Molenar, J. V., Eldred, R. A., and Sisler, J. F.: Examining the relationship among atmospheric aerosols and light scattering and extinction in the Grand Canyon area, J. Geophys. Res. 101, 19251–19265, 1996.

Malm, W. C., Day, D. E., and Kreidenweis, S. M.: Light scattering characteristics of aerosols as a function of relative humidity: Part I – A comparison of measured scattering and aerosol concentrations using the theoretical models, J. Air Waste Manage., 50, 686–700, 2000.

Manktelow, P. T., Mann, G. W., Carslaw, K. S., Spracklen, D. V., and Chipperfield, M. P.: Regional and global trends in sulphate aerosol since the 1980's, Geophys. Res. Lett., 34, L14803, doi:10.1029/2006GL028668, 2007.

Molenar, J. V.: Analysis of the real world performance of the Optec NGN-2 ambient nephelometer, in: Visual Air Quality: Aerosols and Global Radiation Balance, Air and Waste Management Association, Pittsburgh, 243–265, 1997.

Mudelsee, M.: Climate Time Series Analysis, vol. 42 of Atmospheric and Oceanographic Sciences Library, Springer, Heidelberg, 2010.

Müller, T., Nowak, A., Weidensohler, A., Sheridan, P., Laborde, M., Covert, D. S., Marinoni, A., Imre, K., Henzing, B., Roger, J-C., Martins dos Santos, S., Wilhelm, R., Wang, Y-Q., and de Leeuw, G.: Angular illumination and truncation of three different integrating nephelometers: implications for empirical size-based corrections, Aerosol Sci. Technol., 43, 581–586, 2009.

Müller, T., Henzing, J. S., de Leeuw, G., Wiedensohler, A., Alastuey, A., Angelov, H., Bizjak, M., Collaud Coen, M., Engström, J. E., Gruening, C., Hillamo, R., Hoffer, A., Imre, K., Ivanow, P., Jennings, G., Sun, J. Y., Kalivitis, N., Karlsson, H., Komppula, M., Laj, P., Li, S.-M., Lunder, C., Marinoni, A., Martins dos Santos, S., Moerman, M., Nowak, A., Ogren, J. A., Petzold, A., Pichon, J. M., Rodriquez, S., Sharma, S., Sheridan, P. J., Teinilä, K., Tuch, T., Viana, M., Virkkula, A., Weingartner, E., Wilhelm, R., and Wang, Y. Q.: Characterization and intercomparison of aerosol absorption photometers: result of two intercomparison workshops, Atmos. Meas. Tech., 4, 245–268, doi:10.5194/amt-4-245-2011, 2011.

Murphy, D. M., Chow, J. C., Leibensperger, E. M., Malm, W. C., Pitchford, M., Schichtel, B. A., Watson, J. G., and White, W. H.: Decreases in elemental carbon and fine particle mass in the United States, Atmos. Chem. Phys., 11, 4679–4686, doi:10.5194/acp-11-4679-2011, 2011.

Nessler, R., Weingartner, E., and Baltensperger, U.: Adaptation of dry nephelometer measurements to ambient conditions at the Jungfraujoch, Environ. Sci. Technol., 39, 2219–2228, 2005a.

Nessler, R., Weingartner, E., and Baltensperger, U.: Effect of humidity on aerosol light absorption and its implications for extinction and the single scattering albedo illustrated for a site in the lower free troposphere, Aeorosl Sci., 36, 958–972, doi:10.1016/j.jaerosci.2004.11.012, 2005b.

O'Connor, T. C., Jennings, S. G., and O'Dowd, C. D.: Highlights of fifty years of atmospheric aerosol research at Mace Head, Atmos. Res., 90, 338–355, 2008.

Ogren, J. A.: Comment on "Calibration and intercomparison of filter-based measurements of visible light absorption by aerosols", Aerosol Sci. Technol., 44, 589–591, 2010.

Ogren, J. A.: WMO/GAW Standard Operating Procedures for In-Situ Measurements of Aerosol Mass Concentration, Light Scattering and Light Absorption, WMO/GAW, Report#200, Switzerland, 2011.

Perry, K. D., Cahill, T. A., Schnell, R. C., and Harris, J. M.: Long-range transport of anthropogenic aerosols to the National Oceanic and Atmospheric Administration baseline station at Mauna Loa Observatory, Hawaii, J. Geophys. Res., 104, 18521–18533, doi:10.1029/1998JD100083, 1999.

Pozzoli, L., Janssens-Maenhout, G., Diehl, T., Bey, I., Schultz, M. G., Feichter, J., Vignati, E., and Dentener, F.: Re-analysis of tropospheric sulfate aerosol and ozone for the period 1980–2005 using the aerosol-chemistry-climate model ECHAM5-HAMMOZ, Atmos. Chem. Phys., 11, 9563–9594, doi:10.5194/acp-11-9563-2011, 2011.

Putaud, J.-P., Raes, F., Van Dingenen, R., Brüggemann, E., Facchini, M.-C., Decesari, S., Fuzzi, S., Gehrig, R., Hüglin, C., Laj, P., Lorbeer, G., Maenhaut, W., Mihalopoulos, N., Müller, K., Querol, X., Rodriguez, S., Schneider, J., Spindler, G., ten Brink, H., Tørseth, K., Wiedensohler, A.: A European aerosol phenomenology-2: chemical characteristics of particulate matter at kerbside, urban, rural and background sites in Europe, Atmos. Environ., 38, 2579–2595, doi:10.1016/j.atmosenv.2004.01.041, 2004.

Quinn, P. K., Shaw, G., Andrews, E., Dutton, E. G., Ruoho-Airola, T., and Gong, S. L.: Arctic Haze: Current trends and knowledge gaps, Tellus B, 59, 99–114, 2007.

Quinn, P. K., Bates, T. S., Schulz, K., and Shaw, G. E.: Decadal trends in aerosol chemical composition at Barrow, Alaska: 1976–2008, Atmos. Chem. Phys., 9, 8883–8888, doi:10.5194/acp-9-8883-2009, 2009.

Reheis, M. C. and Urban, F. E.: Regional and climatic controls on seasonal dust deposition in the southwestern US, Aeolian Res., 3, 3–21, doi:10.1016/j.aeolia.2011.03.008, 2011.

Roy, B., Mathur, R., Gilliland, A. B., and Howard, S. C.: A comparison of CMAQ-based aerosol properties with IMPROVE, MODIS, and AERONET data, J. Geophys. Res., 112, D14301, doi:10.1029/2006JD008085, 2007.

Sen, P. K.: Estimates of the regression coefficient based on Kendall's tau, J. Am., Stat. Assoc., 63, 1379–1389, 1968.

Seinfeld, J. H. and Pandis, S. N.: Atmospheric Chemistry and Physics, John Wiley and Sons, New York, 1998.

Sharma, S., Andrews, E., Barrie, L. A., and Ogren, J. A.: Variations and sources of the equivalent black carbon in the high Arctic revealed by long term observations at Alert and Barrow: 1989–2003, J. Geophys. Res., 111, D14208, doi:10.1029/2005JD006581, 2006.

Sharma, S., Chan, E., Ishizawa, M., Toom-Sauntry, D., Gong, S. L., Li, S. M., Tarasick, D. W., Leaitch, W. R., Norman, A., Quinn, P. K., Bates, T. S., Levasseur, M., Barrie, L. A., and Maenhaut, W.: Influence of transport and ocean ice extent on biogenic aerosol sulfur in the Arctic atmosphere, J. Geophys. Res., 117, D12209, doi:10.1029/2011JD017074, 2012.

Sisler, J. F. and Malm, W. C.: The relative importance of soluble aerosols to spatial and seasonal trends of impared visibility in the United States, Atmos. Environ., 28, 851–862, 1994.

Sirois, A.: A brief and biased overview of time-series analysis of how to find that evasive trend, WMO/EMEP Workshop on Advanced Statistical Methods and Their Application to Air Quality Data Sets, Annex E., Global Atmosphere Watch No. 133, TD-No. 956, World Meteorological Organization, Geneva, Switzerland, 1998.

Sorooshian, A., Wonaschütz, A., Jarjour, E. G., Hashimoto, B. I., Schichtel, B. A., and Betterton, E. A.: An aerosol climatology for a rapidly growing arid region (southern Arizona): Major aerosol species and remotely sensed aerosol properties, J. Geophys. Res., 116, D19205, doi:10.1029/2011JD016197, 2011.

Spracklen, D. V., Carslaw, K. S., Merikanto, J., Mann, G. W., Reddington, C. L., Pickering, S., Ogren, J. A., Andrews, E., Baltensperger, U., Weingartner, E., Boy, M., Kulmala, M., Laakso, L., Lihavainen, H., Kivekäs, N., Komppula, M., Mihalopoulos, N., Kouvarakis, G., Jennings, S. G., O'Dowd, C., Birmili, W., Wiedensohler, A., Weller, R., Gras, J., Laj, P., Sellegri, K., Bonn, B., Krejci, R., Laaksonen, A., Hamed, A., Minikin, A., Harrison, R. M., Talbot, R., and Sun, J.: Explaining global surface aerosol number concentrations in terms of primary emissions and particle formation, Atmos. Chem. Phys., 10, 4775–4793, doi:10.5194/acp-10-4775-2010, 2010.

Stjern, C. W., Stohl, A., and Kristjansson, J. E.: Have aerosols affected trends in visibility and precipitation in Europe?, J. Geophys. Res., 116, D02212, doi:10.1029/2010JD014603, 2011.

Streets, D. G., Yan, F., Chin, M., Diehl, T., Mahowald, N., Schultz, M., Wild, M., Wu, Y., and Yu, C.:Anthropogenic and natural contributions to regional trends in aerosol optical depth, 1980–2006, J. Geophys. Res., 114, D00D18, doi:10.1029/2008JD011624, 2009.

Tørseth, K., Aas, W., Breivik, K., Fjæraa, A. M., Fiebig, M., Hjellbrekke, A. G., Lund Myhre, C., Solberg, S., and Yttri, K. E.: Introduction to the European Monitoring and Evaluation Programme (EMEP) and observed atmospheric composition change during 1972–2009, Atmos. Chem. Phys., 12, 5447–5481, doi:10.5194/acp-12-5447-2012, 2012.

VanCuren, R. A. and Cahill, T. A.: Asian aerosols in North America: Frequency and concentration of fine dust, J. Geophys. Res., 107, 4804, doi:10.1029/2002JD002204, 2002.

Van Dingenen, R. , Raes, F., Putaud, J.-P., Baltensperger, U., Charron, A., Facchini, M.-C., Decesari, S., Fuzzi, S., Gehrig, R., Hansson, H.-C., Harrison, R.M., Hüglin, C., Jones, A.M., Laj, P., Lorbeer, G., Maenhaut, W., Palmgren, F., Querol, X., Rodriguez, S., Schneider, J., ten Brink, H., Tunved, P., Tørseth, K., Wehner, B., Weingartner, E., Wiedensohler, A., and Wåhlin, P.: A European aerosol phenomenology-1: physical characteristics of particulate matter at kerbside, urban, rural and background sites in Europe, Atmos. Environ., 38, 2561–2577, doi:10.1016/j.atmosenv.2004.01.040, 2004.

Wang, X. L. and Swail, V. R: Changes of extreme wave heights in Northern Hemisphere oceans and related atmospheric circulation regimes, J. Climate, 14, 2204–2221, 2001.

Weatherhead, E. C., Reinsel, G. C., Tiao, G. C., Meng, X.-L., Choi, D., Cheang, W.-K., Keller, T., DeLuisi, J., Wuebbles, D. J., Kerr, J. B., Miller, A. J., Oltmans, S. J., and Frederick, J. E.: Factors affecting the detection of trends: Statistical considerations and applications to environmental data, J. Geophys. Res., 103, 17149–17161, doi:10.1029/98JD00995, 1998.

Weatherhead, E. C., Reinsel, G. C., Tiao, G. C., Jackman, C. H., Bishop, L., Hollandsworth, F. S. M., DeLuisi, J., Keller, T., Oltmans, S. J., Flemming, E. L.,Wuebbles, D. J., Kerr, J. B., Miller, A. J., Herman, J., McPeters, R., Nagatani, R. M., and Frederick, J. E.: Detecting the recovery of total column ozone, J. Geophys. Res., 105, 22201–22210, 2000.

Weingartner, E., Saathoff, H., Schnaiter, M., Streit, N., Bitnar, B., and Baltensperger, U.: Absorption of light by soot particles: determination of the absorption coefficient by means of aethalometers, Aerosol Sci., 34, 1445–1463, 2003.

Weller, R., Wagenbach, D., Legrand, M., Elsässer, C., Tian-Kunze, X., and König-Langlo., G.: Continuous 25-years aerosol records at coastal Antarctica: 1. Inter-annual variability of ionic compounds and links to climate indices, Tellus B, 63, 044011, doi:10.1111/j.1600-0889.2011.00542.x, 2011.

Westerling, A. L., Hidalgo, H. G., Cayan, D. R., and Swetnam, T. W.: Warming and earlier spring increase western US forest wildfire activity, Science, 313, 940–943, 2006.

Wiedensohler, A., Birmili, W., Nowak, A., Sonntag, A., Weinhold, K., Merkel, M., Wehner, B., Tuch, T., Pfeifer, S., Fiebig, M., Fjäraa, A. M., Asmi, E., Sellegri, K., Depuy, R., Venzac, H., Villani, P., Laj, P., Aalto, P., Ogren, J. A., Swietlicki, E., Williams, P., Roldin, P., Quincey, P., Hüglin, C., Fierz-Schmidhauser, R., Gysel, M., Weingartner, E., Riccobono, F., Santos, S., Grüning, C., Faloon, K., Beddows, D., Harrison, R., Monahan, C., Jennings, S. G., O'Dowd, C. D., Marinoni, A., Horn, H.-G., Keck, L., Jiang, J., Scheckman, J., McMurry, P. H., Deng, Z., Zhao, C. S., Moerman, M., Henzing, B., de Leeuw, G., Löschau, G., and Bastian, S.: Mobility particle size spectrometers: harmonization of technical standards and data structure to facilitate high quality long-term observations of atmospheric particle number size distributions, Atmos. Meas. Tech., 5, 657–685, doi:10.5194/amt-5-657-2012, 2012.

Wild, M.: Global dimming and brightening: A review, J. Geophys. Res., 114, D00D16, doi:10.1029/2008JD011470, 2009.

Wild, M.: Enlightening global dimming and brightening. Bull. Amer. Meteor. Soc., 93, 27–37, doi:10.1175/BAMS-D-11-00074.1, 2012.

Xia, X. G.: Variability of aerosol optical depth and Angstrom wavelength exponent derived from AERONET observations in recent decades, Environ. Res. Lett., 6, 044011 , doi:10.1088/1748-9326/6/4/044011, 2011.

Yoon, J., von Hoyningen-Huene, W., Kokhanovsky, A. A., Vountas, M., and Burrows, J. P.: Trend analysis of aerosol opti-

cal thickness and Ångström exponent derived from the global AERONET spectral observations, Atmos. Meas. Tech., 5, 1271–1299, doi:10.5194/amt-5-1271-2012, 2012.

Yu, F., Luo, G., Turco, R. P., Ogren, J. A., and Yantosca, R. M.: Decreasing particle number concentrations in a warming atmosphere and implications, Atmos. Chem. Phys., 12, 2399–2408, doi:10.5194/acp-12-2399-2012, 2012.

Yue, S., Pilon, P., Phinney, B., and Cavadias, G.: The influence of autocorrelation on the ability to detect trend in hydrological series, Hydrol. Process., 16, 1807–1829, doi:10.1002/hyp.1095, 2002.

Zhang, J. and Reid, J. S.: A decadal regional and global trend analysis of the aerosol optical depth using a data-assimilation grade over-water MODIS and Level 2 MISR aerosol products, Atmos. Chem. Phys., 10, 10949–10963, doi:10.5194/acp-10-10949-2010, 2010.

Zhang, X. and Zwiers, F. W.: Comment on "Applicability of prewhitening to eliminate the influence of serial correlation on the Mann-Kendall test" by Sheng Yue and Chun Yuan Wang, Water Resour. Res., 40, W03805, doi:10.1029/2003WR002073, 2004.

Zhang, Q., Jimenez ,J. L., Canagaratna, M. R., Allan, J. D., Coe, H., Ulbrich, I., Alfarra, M. R., Takami, A., Middlebrook, A. M., Sun, Y. L., Dzepina, K., Dunlea, E., Docherty, K., DeCarlo, P. F., Salcedo, D., Onasch, T., Jayne, J. T., Miyoshi, T., Shimono, A., Hatakeyama, S., Takegawa, N., Kondo, Y., Schneider, J., Drewnick, F., Weimer, S., Demerjian, K., Williams, P., Bower, K., Bahreini, R., Cotrell, L., Griffin, R. J., Rautiainen, J., Sun, J. Y., Zhang, Y. M., and Worsnop, D. R.: Ubiquity and dominance of oxygenated species in organic aerosols in anthropogenically-influenced Northern Hemisphere mid-latitudes, Geophys. Res. Lett., 34, L13801, doi:10.1029/2007GL029979, 2007.